POLITECNICO DI MILANO

Scuola di Ingegneria Industriale e dell'Informazione

Corso di Laurea Magistrale in Ingegneria Elettrica

Probabilistic Production Simulation Including Wind Farms Based on Equivalent Interval-Frequency Distribution

Relatore: Prof. Alberto Berizzi

Tesi di Laurea Magistrale di:
Jin Lanju
Matr. 10431698

Anno Accademico 2014-2015

ABSTRACT

Abstract in italiano

La tradizionale simulazione probabilistica di produzione dei sistemi elettrici di potenza si basa sulla curva di durata del carico per descrivere le propriet àtemporali del carico. Tuttavia, questa descrizione manca delle informazioni sulle fluttuazioni del carico e dei vincoli temporali relativi alla caratteristica cronologica, ci ò si traduce nel fatto che non tiene conto dei tempi minimi e massimi, delle restrizioni sulle rampe, dell'organizzazione dei generatori e di altri fattori nel processo di simulazione. Il metodo tradizionale non è in grado valutare il costo dinamico di avvio e di arresto delle unit àcausato dalla fluttuazione del carico e di conseguenza la valutazione risulta relativamente approssimata. Con la crescente diffusione delle tecnologie non programmabili, come l'eolico, la crescente fluttuazione di carico produrrà un impatto maggiore. Pertanto abbiamo bisogno urgentemente di studiare la simulazione probabilistica di produzione che èin grado di fornire una valutazione pi ùglobale.

Il metodo di frequenza e durata (FD) impiega la curva di frequenza di carico per rispecchiare i fattori di fluttuazione sopracitati, corrispondenti alla frequenza di operazioni di avvio e di arresto delle unità. Tuttavia FD ignora l'impossibilita di avvio e arresto negli intervalli brevi di tempo, portando cosi ad uno scostamento nel risultato. Al fine di riflettere maggiormente le caratteristiche cronologiche del carico e ottenere un risultato pi ù realistico, in questa tesi la curva di frequenza di carico è estesa alla distribuzione degli intervalli di frequenza e alla serie della distribuzione degli intervalli di frequenza, che coinvolge sia le informazioni sulla frequenza sia le informazioni sulla distribuzione temporale delle fluttuazioni del carico. Pi ù dettagliatamente, la frequenza di transizione di ogni livello di carico viene espansa in una serie di intervalli temporali, utilizzando una struttura di tempo per registrare ciascun intervallo adiacente di tempo di trasferimento. Poi, analogamente alla derivazione delle curve di durata del carico effettivo (ELDCs) nei costi Bleriaux-Booth, la distribuzione di frequenza dei carichi effettivi, con le informazioni dei rispettivi intervalli di tempo, pu ò essere valutata con il processo di convoluzione, che pu ò essere considerato come una modifica di ogni struttura temporale. In questo modo, viene sviluppato il metodo di simulazione di produzione probabilistico basato sull'equivalente distribuzione di intervalli di frequenza. Le informazioni

cronologiche sia dei carichi che dei parchi eolici possono essere coinvolte, in una certa misura, sulla base delle informazioni di intervallo di tempo delle strutture temporali effettive. In più, l'effetto dell'energia eolica viene valutato più ragionevolmente per quanto riguarda i costi dinamici.

L'impatto dei parchi eolici sull'affidabilità metrica, più olistiche informazioni di costo comprensivo del costo del carburante, costi ambientali e costi dinamici saranno discussi con l'algoritmo presentato e il sistema di test integrato EPRI-36 per l'eolico. Anche l'impatto dell'energia eolica sui costi dinamici è studiato. Esempi numerici dimostrano che questo tipo di algoritmo è più vicino alla realtà e più accurato rispetto ai metodi FD.

Abstract in inglese

The traditional probabilistic production simulation of power system is based on the load duration curve to describe the temporal property of the load. However, this derived description misses the load fluctuation information and time constraints related to the chronological characteristic, which is resulting in the fact that it fails to take consideration of the minimum up time and minimum down time limit, ramping rate restriction, generator scheduling, and other factors in the production simulation process. The traditional way can not evaluate the dynamic cost of unit startup and shutdown caused by the load fluctuation and the assessment is relatively rough as a result. With the increasing penetration of non-dispatchable technologies, such as the wind power, more impact will be produced by the growing fluctuation of net load. Therefore urgently we need to study the probabilistic production simulation which can provide a comprehensive assessment.

The frequency and duration (FD) method employes the load frequency curve to reflect the above fluctuation factors, corresponding to the frequency of unit startup and shutdown operation. But it ignores the infeasibility of the startup and shut down in short time interval, which also leads to a deviation in the result. In order to reflect more chronological load characters and get a more realistic result, in this thesis the load frequency curve is extended to the interval frequency distribution and interval frequency distribution series, which involves

both the frequency information and time distribution information of load fluctuation. In more details, the transition frequency of every load level is expanded into a time interval series, by using a time structure to record each time interval of adjacent upward transfer and downward transfer. Then analogously to the derivation of Effective Load Duration Curves (ELDCs) in Bleriaux-Booth costing, the effective load interval frequency distribution function with the information of respective time interval can be evaluated through the convolution process, which can be regarded as a modification of each time structure. In this way, the probabilistic production simulation method based on the equivalent interval frequency distribution is developed. The chronological information of both the load and wind farms can be involved to a certain extent based on the time interval information of effective time structures. What's more, the effect of wind power is also evaluated more reasonably with the respect to the dynamic cost.

With the presented algorithm and the wind power integrated EPRI-36 test system, the impact of the wind farms on reliability metric and more holistic cost information including fuel cost, environmental cost and dynamic cost will be discussed, and the impact of the wind power scale on dynamic cost rate is also studied. Numerical examples demonstrates that this kind of algorithm is more close to reality and more accurate compared to the FD methods.

List of Main Symbols

m	The upward load transfer duration [h]
n	The downward load transfer duration [h]
$a_{(k,m,n)}$	The first type of time structure which indicates the upward transfer frequency of load level *k*, of which the front and back adjacent time interval is *m* and *n*, respectively
$b_{(k,n,m)}$	The second type of time structure which indicates the downward transfer frequency of load level *k*, of which the front and back adjacent time interval is *n* and *m*, respectively
$A_{K\times M\times N}$	The first type of interval-frequency distribution series made up of time structure $a_{(k,m,n)}$
$B_{K\times N\times M}$	The second type of interval-frequency distribution series made up of time structure $b_{(k,n,m)}$
$IF(k)$	The whole combined interval-frequency distribution series of load level *k*
Δx	The load step in the simulation process
I	The total number of units
K	The corresponding discrete values of maximum load in the initial system
C_i	The capacity of *i-th* unit
K_i	The corresponding discrete values of *i-th* unit capacity, $K_i = C_i / \Delta x$
J_{i-1}	The loading position for *i-th* unit, $J_{i-1} = \sum_{j=1}^{i-1} C_j \Big/ \Delta x$
J_I	The discrete value of total installed capacity, $J_I = \sum_{j=1}^{I} C_j \Big/ \Delta x$
$IF_e^{(i-1)}(k)$	The equivalent interval-frequency distribution series after arranging the first *i-1* units
$a_{(k,m,n)}^{i-1}$	The first equivalent time structure of the interval-frequency distribution after loading the perivous *i-1* units
$b_{(k,n,m)}^{i-1}$	The second equivalent time structure of the interval-frequency distribution after loading the perivous *i-1* units
$m_{\min}^{i}$	The minimum up time of *i-th* unit

$n_{\min}^{i}$	The minimum down time of *i-th* unit
F_i^{start}	The expected startup frequency of *i-th* unit
F_i^{end}	The expected shutdown frequency of *i-th* unit
T_i^{start}	The expected removed startup frequency of *i-th* unit
T_i^{end}	The expected removed shutdown frequency of *i-th* unit
I_{FGSUC}	The generator startup and shutdown of unit capacity, $I_{FGSUC} = \dfrac{\frac{1}{T}\sum_{i=1}^{I} C_i \left(F_i^{start} + F_i^{end} \right)}{\sum_{i=1}^{n} C_i}$
I_{STIPUC}	The Short Time Interval Proportion of Unit Capacity $I_{\mathrm{STIPUC}} = \dfrac{\frac{1}{T}\sum_{i=1}^{I} C_i \left(T_i^{start} + T_i^{end} \right)}{\sum_{i=1}^{n} C_i}$
I_{STIDC}	The short time interval dynamic cost

Index of Figures

Index of Tables

Contents

1 Preface

1.1 Background and Motivation

In today's society with the increasing environmental conditionality and decreasing natural resources. The market-oriented reforms of power industry is in a accelerating process. For the formulation of effective planning, how to take full consideration of power supply structure optimization adjustment is the key point in energy saving electricity production with higher requirements so that it can provide a great decisive and policy support for the power industry more scientific, efficient, economic, sustainable, coordinated development.

Recently China's power industry is develop rapidly. The annual growth rate of power generator installed capacity and power generation is reaching 10.5% and 10.34%, respectively. The current total installed capacity is ranking in the second place in the world, just after the United States [2]. However, the production of electricity is mainly through coal, in which the coal-fired electricity generation is accounting for about 75% and the numerous fossil fuel consumption and heavy environment pollution is becoming a great bottleneck, severely restricting China's economic growth. To adjust and optimize the energy structure, exploring new energy sources and recycling energy, is an important security and energy sustainability policy for healthy development. Wind power is belonging to a kind of renewable energy, which is also favorable to environmental protection. Not only it does not require to burn fossil fuels, but also it will not cause any air pollution. Therefore, more and more attention is taken in the research of wind power around the world. Meanwhile, wind power has a huge reserve. According to the incomplete statistics, the total global wind resource is not less than 2.74×10^{6}GW, of which, for the development and utilization of wind energy is accounting for 2×10^{4}GW. China's wind energy reserve is distributed in a wide area, merely it has approximately 2.53×10^{2}GW on land, indicating a bright development potential and prospect. In today’s society, the problem of environmental pollution and energy sustainability is growing more serious. Meanwhile the electricity market is in the gradual deepening of reform. The utilization of renewable energy for power generation in the world have become a hot topic, and also have a rapid development, especially, for the wind power, it is one of the fastest growing power generations and it is also the most mature and advanced at the technical level.

During the "Eleventh Five Year Plan", China's wind power has been developed rapidly [2]. According to official statistics, our total installed capacity of wind power in 2013 is already reached as much as 74.58GW and it is increased into 90GW, of which wind power generating capacity is 15.63 billion kwh, with an increase by 12.2% [6]. Wind power equipment utilization hours are as high as 1905 hours. In addition, there is an ambitious objective for the development of the new energy source in future. By 2020, the wind power capacity will plan to increase from 30GW to 150GW. Among them, the Jiangsu wind power base of million kilowatts in 2015 has the installed capacity of 3.8GW [3], and the target for 2020 target is to improve into 10GW of wind power capacity. Jiuquan wind power base of million kilowatts in 2011 has the installed capacity of 4.201GW [5], and it is planned to reach 12.71GW in the "Twelfth five Year Plan", which will become one of the world's largest wind power bases. Table 1-1 shows eight 10GW wind power bases under planning and construction from the National Development and Reform Commission [7]. In 2020, the total capacity of these eight wind power bases will exceed 120GW.

Table 1-1 Planning and construction of wind power bases

Location	Planned capacity [GW]	Grid to be connected
Gansu Jiuquan	12	Northwest Grid
Xinjiang Hami	20	Northwest Grid
Mongolia west	20	North China Grid
Mongolia east	30	Northeast Grid
Hebei north	10	North China Grid
Jiangsu	10	East China Grid
Jilin	10	Northeast Grid
Shandong	15	North China Grid

While the wind power penetrates the power system for its clean and renewable benefits, its effect on the aspects of power system operation and planning will become increasingly prominent. Due to the stochastic volatility of the wind power, not only the reverse power pressure is enlarged, but also the startup and shutdown operations of conventional units to meet the fluctuated net loads are becoming more frequently, which leads to increment of relevant dynamic costs. Moreover, the wind farm output at night is generally greater than that one during the day, also greater in winter more than one in summer, which is just exactly the

opposite to the normal changing law of system load. What is worse, wind turbines have a poor control and this anti-peaking property is likely to increase the equivalent gap of the peak and valley load. All in all, the high volatility and intermittency of wind power output is bring new difficulties to the entire power system dispatch, probably making the system operation further deteriorate.

Reference [8] and [9] employed the measured data in the Jiuquan wind power base to study the wind power output characteristics and note that the wind power output has obvious relevance and require more conventional power generators for peaking plan, considering from the long time scales. Reference [10] pointed that after the wind power with 5160MW installed capacity access the Gansu Power Grid, the gap between the peak load and valley load became almost three times of that one without wind power. The monthly average peak-valley difference rate in Gansu power grid 2010 is close to or exceeds the maximum regulating peak load ability in the case when the thermal power generators are not allowed to startup and shutdown in one day. Hence, the coordination of the conventional unit startup and shutdown and the peak regular is becoming significantly frequently in the power system including wind farms, which will definitely increase a lot in the dynamic cost of consumption. Wind power penetration will extremely increase the additional cost. Accordingly, the impact of wind power on the power system cannot be ignored and we need to make the scientific and rational deployment planning to develop these renewable energy sources.

As one of the significant methods for improvement and optimization of power system production, stochastic production simulation is comprehensively considering both of the load variation and random generator fault for the calculation of production costs and reliability analysis, under the optimal operation based on the predicted future load curve. Its core mission is to carry on operating mode analysis, production cost calculation and reliability evaluation. Basic functions can be broadly grouped into the following aspects [19]:

(1) provide the expected production energy for each plant, the fuel consumption and the corresponding fuel costs during the simulation under optimum operating mode;

(2) compute power system reliability indicators in this operating mode, for example, the Expected Energy Not Supplied (EENS) and the Loss of Load Probability (LOLP);

(3) analyze the whole production cost in this simulation, including the environmental cost, the customer interruption cost and so on.

Stochastic production simulation is playing an important role in assessing the future development of the power system to improve economic efficiency and supply reliability level of power system operation. As an important way to evaluate the reliability and production cost, it is quite necessary to consider the impact brought by wind power volatility. If the timing information of wind power can be also modeled in the processing, it will help to get a more accurate evaluation with a full point of view.

1.2 Status of Production Simulation with wind power

As for the production simulation for power system, domestic and foreign scholars already have done a lot of research, which generally can be divided into two types of simulation model-- stochastic production simulation and probabilistic production simulation [22].

Stochastic production models is simulating directly in the chronological load curve. The main method is called Monte Carlo and Markov [16]. Through detailed statistics of frequency of each incident, Monte Carlo can make the deep estimation of system state. However, the convergence speed is proportional to the square root of sample size, resulting in a large computation and certain randomness, which limits the widespread use of such methods. The core of probabilistic production simulation is to transform the timing load curve into the Load Duration Curve (LDC) and the effect of random outages of generating units is considered as the increase of system load to form the equivalent load duration curve. It reflects that after the unit is outage with certain probability, the rest of other units will face a relatively large equivalent load duration curve, namely, to bear more load. Probabilistic model was first introduced by Baleriaux in the 60s [15], Booth continued to improve it, thereby the famous Baleriaux-Booth model and algorithm were formed, of which the key is to convolute standardly the probabilistic random variables of distribution function in the simulation. Around how to describe the timing load curve and how to improve the speed and accuracy of convolution and deconvolution calculation, scholars made a lot of improvements. Typical algorithms are [19]: Piecewise Linear Approximation Method, the Cumulant Method [17], the Method of Moments [18], Mixture of Normal Approximation Method (MONA), Fast Fourier Transform Method (FFT) and Equivalent Energy Function (EEF) [20] [21] and so on.

However, the load duration curve lose part of timing information of system load and can not include the time-dependent constraints, such as unit commitment fee, the minimum time requirement of startup and shutdown, ramp rate constrain of thermal power units, etc. The

conventional unit startup and shutdown cost, hot standby and other dynamic characteristics and dynamic cost are not taken into consideration in the simulation process, leading to the sad fact that production costs are relatively sketchy.

Extensive literatures [10]-[12] discussed the establishment of the wind farm model reliability or peaking related strategies, but for wind power planning including economic evaluation of unit startup and shutdown, power reserves and peaking regulation, it is poorly studied. When penetrating large-scale wind power under priority consumptive principle, the system load volatility is strengthened a lot and the peak-valley difference is also growing, which means a corresponding increase in conventional unit startup and shutdown operation and dynamic cost. How to assess the dynamic cost so as to make the power planning run into a meaningful surface for a comprehensive analysis of the production costs, evaluation of the wind farm effectiveness and determination of wind power capacity is quite crucial. The traditional simulation algorithm is no longer able to meet the practical requirements of the power system in the production cost assessment to a certain degree.

Literatures [33]-[38] proposed a method based on the load frequency curve, namely Frequency and Duration Method (FD). It employs the load frequency curve (LFC) instead of the load duration curve to describe the load timing characteristics to consider more timing related information. Among them, the literature [37] and [38] combine the EEF method with the load frequency curve to evaluate the production simulation. The FD method reflects part of the timing fluctuation of frequency information, but at the same time it misses the timing distribution fluctuations, causing that the dynamic costs of startup and shutdown in short time interval in the simulation process is also included when assessing the whole production costs. It fails to accord with the practical operations and introduces a potentially significant bias inaccuracy in assessment. With the increasing penetration of non-dispatchable technologies, such as the wind power, this error will become more apparent.

1.3 Main Contents of the Study

In order to reflect more chronological load characteristics for a more reasonable dynamic cost, this thesis introduces the interval frequency distribution series based on load transfer(hereinafter referred to as the interval-frequency distribution), as an extension of load frequency curve. Composed of time structures, the interval-frequency distribution not only contains all the information in the load frequency curve, but also to a certain extent reflect the

timing distribution of load fluctuation, providing more basis when assessing the dynamic cost of unit startup and shutdown caused by the penetration of wind power. A new probabilistic production costing is studied just based on this new description of load curve. Specific work completed in this thesis is as follows.

(1) for the time-varying characteristics of the load, the load frequency curve will extend into the load beyond the interval-frequency distribution in the form of time structure, not only to cumulate the number of load transfers, but also to maintain recording two adjacent time intervals of each load transfer, reflecting both the timing fluctuation frequency information and time distribution of information.

(2) Analog to frequency and duration curve, develop the new probabilistic production simulation algorithm based on the establishment of equivalent interval-frequency distribution. By standard convolution, the random failure influence of unit is considered as the continually updated equivalent interval-frequency distribution series of the previous one. Based on the detailed information contained in each corrected time interval, the expected power generation, system reliability, the frequency of unit startup and shutdown and related dynamic costs are respectively elaborated in the evaluation system.

(3) Combined with EPRI-36 system and the IEEE RTS, simulate the production in the first 30 days of one month with proposed method, where the wind farm refers to the historical data of Da Ban Cheng region. Assess the production cost based on the equivalent interval-frequency distribution. Then analyze and compare the results with the one in equivalent energy function method, frequency and duration method to verify the validity and accuracy of the proposed method. Finally, the influence of the wind power penetrated scale on the entire power system will be also studied.

2 The Extension Principle of Load Interval-Frequency Distribution Series

2.1 Brief Introduction

Power System Probabilistic Production Simulation is a kind of algorithm, which is based on considering both random failures of units and the system load fluctuation, aiming to calculate the expected energy for each plant, the production costs and system reliability indices in the optimum operating mode. As it is well-known, the timing fluctuation of system load leads to the startup and shutdown operations of units to balance the whole system, which will result in the so-called dynamic costs. With the increasing amounts of intermittent energy access, the volatility of the system will be further improved and the dynamic operation of the conventional units will become more frequent. Timing fluctuations information is including both the fluctuated frequency and the distribution of the fluctuation. If these information is more completed reflected in the simulation, it will help a lot to characterize and describe some relevant phenomena. Therefore, how to accurately describe the load characteristics and give a full consideration to the timing fluctuation of the system is one of the key issues to get a comprehensive assessment of probabilistic production simulation.

2.2 Load Duration Curve and Load Frequency Curve

Generally speaking, the chronological load curve in the traditional method is converted into the duration curve to describe the characteristics of system load. Instead by the time increments, the duration curve is ordered by the duration of each load level in the whole study period. Depending on the study period, it can be classified into daily, weekly, monthly, and annual duration curve. Fig. 2-1 shows the relationship between the daily load curve and the corresponding duration load curve, and the time relation in *x* axis of each load level is always satisfying the formula (2-1).

$$t'_i = \sum_j t_{ij} \tag{2-1}$$

Where:

t_{ij} ——the *j-th* duration of load P_i in the chronological load curve;

t'_i——the total duration of load P_i .

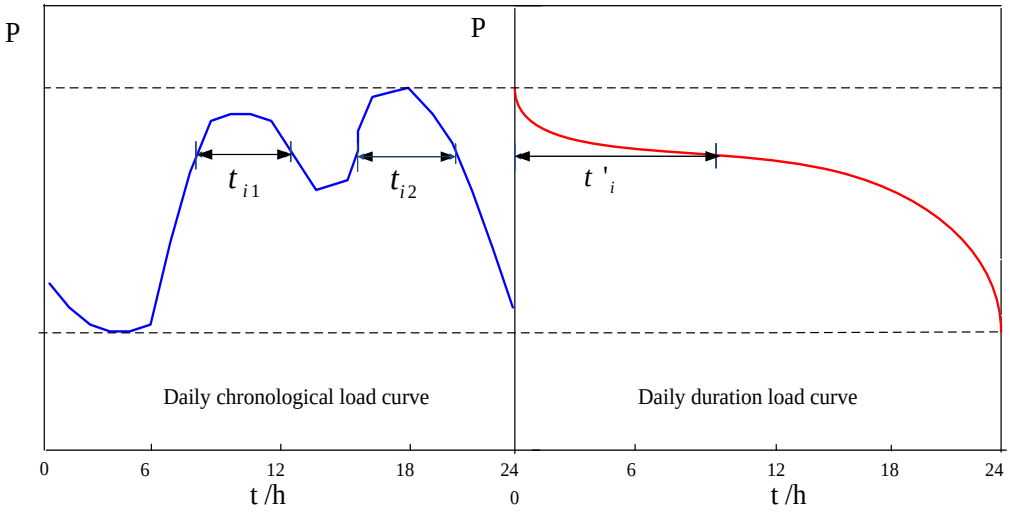

Fig. 2-1 Daily duration load curve

For example, in Fig. 2-1, there exists this kind of relationship, $t'_i = t_{i1} + t_{i2}$. Typically, the duration load curve can be obtained by rotating these two coordinates in Fig. 2-1. As shown in the Fig. 2-2, which presents a daily duration load curve, the *x* axis means the load level and the *y* axis represents the corresponding duration. T means the study period, $P_{L\max}$ is the maximum load for the system. At any point (*x*, *t*) in the curve, it indicates the duration of system load which is equal or greater than *x* is equal to *t*, i.e.,

$$t = F(x) \tag{2-2}$$

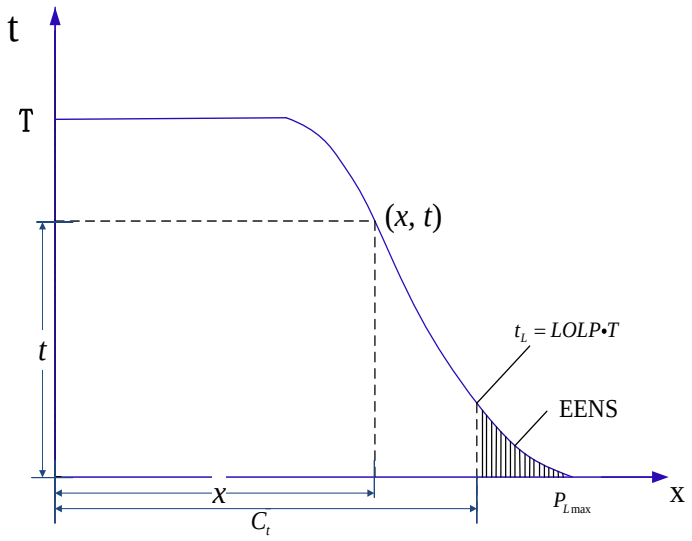

Fig. 2-2 Duration load curve explaination

Obviously, such derived method above would result in loss of part of load time

information, such as the load fluctuation information, making it impossible to involve the related dynamic costs of generator count in probabilistic production simulation. Fig. 2-3(a) shows two different timing load curve $L_1(x)$ and $L_2(x)$, converting into the load duration curve using the method above, both of these two duration load curves are exactly the same [37], as shown in Fig. 2-3(b). However, there is no doubt that the fluctuation frequency and amplitude of the load curve $L_2(x)$ is much larger than the load curve $L_1(x)$. Obviously, the startup and shutdown operations of unit with $L_2(x)$ system is more frequently and it costs more in the aspect of warm-up, maintaining the operating reserve which is related to the dynamic factors.

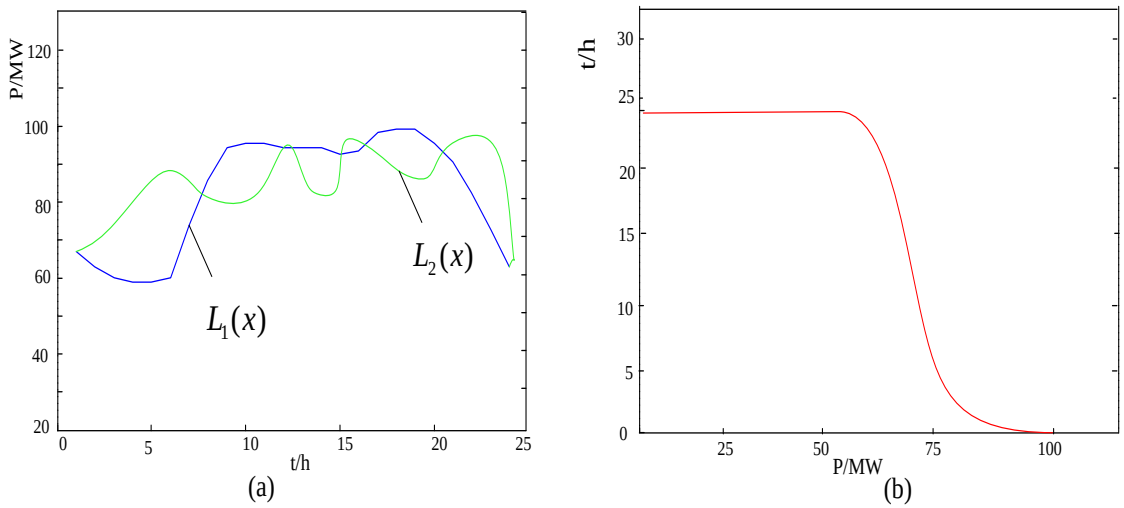

Fig. 2-3 Daily chronological load curve and its duration load curve

The load frequency curve is firstly introduced to regard the chronology of events. It represents the average frequency in the study period with which load level is crossed in an upward direction of the chronological curve, i.e., the load is in transition from lower one to higher one. What's more, it's exactly equal to the average frequency with which load level is crossed in an downward direction. Assume that σ is the average times of upward cross of load level *k*, then its corresponding load frequency $f_L(k)$ is

$$f_L(k)=\frac{\sigma}{T} \tag{2-3}$$

Fig. 2-4 illustrates one typical day (24h) load data that includes the original load, wind power output and net load. Take the example of load level of 6000MW. Scanning the load curve from the beginning in the original load curve, the load is 5516MW at 7:00 and increases to 6182MW at 8:00. And the upward transfer happens only once over the study period.

Therefore, the original frequency in the 6000MW load level is 1/24. Similarly, all the other load frequency can be obtained in this way and the corresponding original load frequency curve is shown in Fig. 2-5, where *x* axis is the system load and *y* axis is corresponding load transfer times. By subtracting the initial load from the intermittent wind power output to consider the impact of intermittent energy sources, we can get the net load curve as the basis of generation of original load frequency curve. Compared with the original load curve in Fig. 2-4, the net load curve obviously has more volatility and in the corresponding load frequency curve, the total load transfer frequency is significantly increased, at the same time the mainly distributed load interval is also changed.

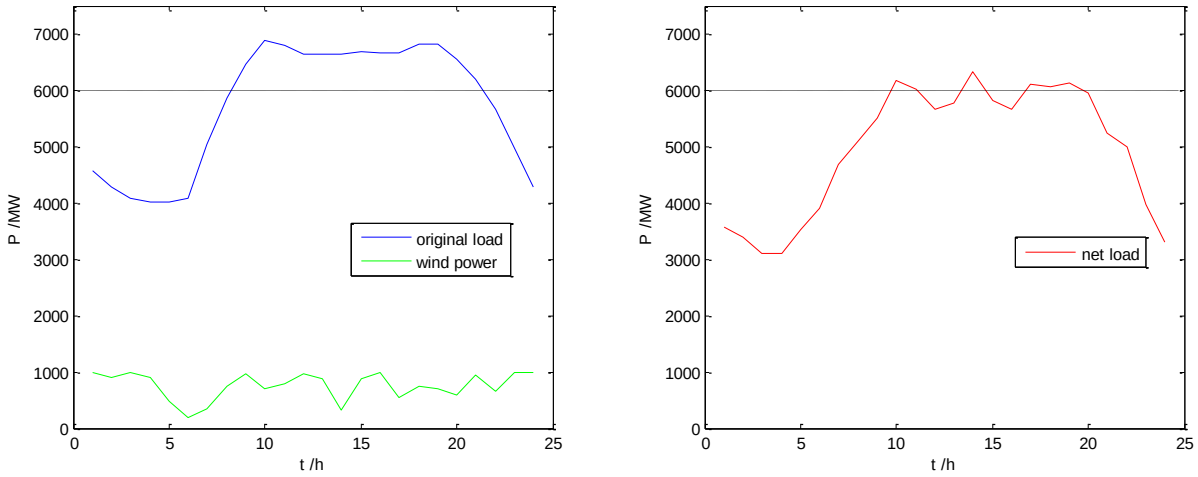

Fig. 2-4 24h original load, net load and wind power

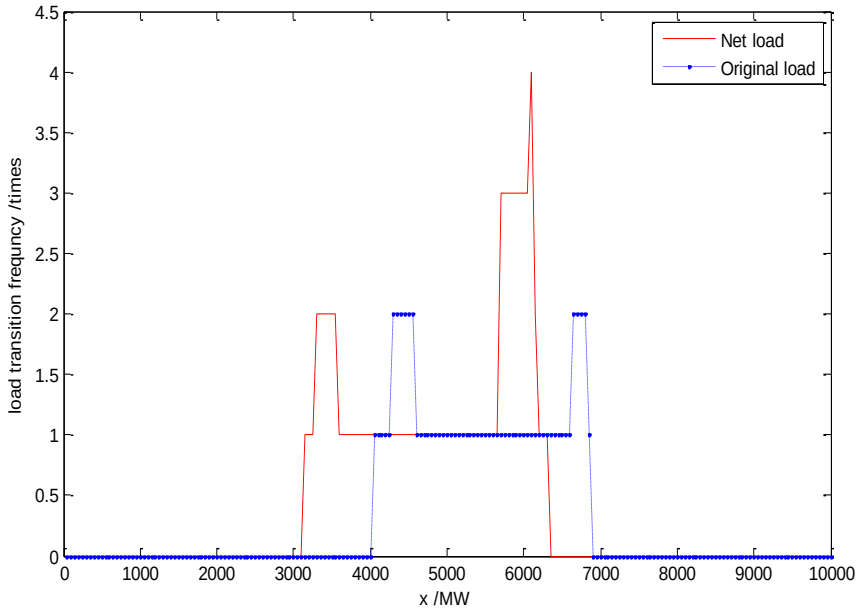

Fig. 2-5 The comparision of the load frequency curve

The Frequency and Duration method is using load frequency curve to reflect the partial load timing information. And through convolution, the equivalent load frequency curve is obtained to correspond the frequency information of the unit startup and shutdown, hence in that way the related dynamic costs are evaluated. Fig. 2-6 illustrates the principle about how the load frequency curve responds to conventional unit commitment. Suppose unit N is loading at the load level 6000MW, the system load is less than 6000MW before 8:00 without accessing the wind power, obviously this unit N is in shutdown state or hot standby. However, when the system load is growing greater than 6000MW after 8:00, accordingly this units N should be switched on, that is to say, the load upward shift corresponds to one time of startup process. Also, before 22:00, since the system load is always greater than 6000MW, where unit N will have to keep on. Until after 22:00, the system load decreases, this unit will be shut down or reduce output to keep a hot spare.

In the FD method, the load frequency curve directly reflects the demand of unit startup and shutdown. When the corresponding loading level is transferring upward, it means the desired unit starts while when the load level is downward transferring, the unit shutdown will be issued. Obviously, the FD method does not take into account the feasibility of continuous startup and shutdown in the short interval, which will introduce a lot of error compared with the actual situation. With the increasing of the intermittent energy access, the system volatility will be further improved and this kind of phenomenon is becoming more notable.

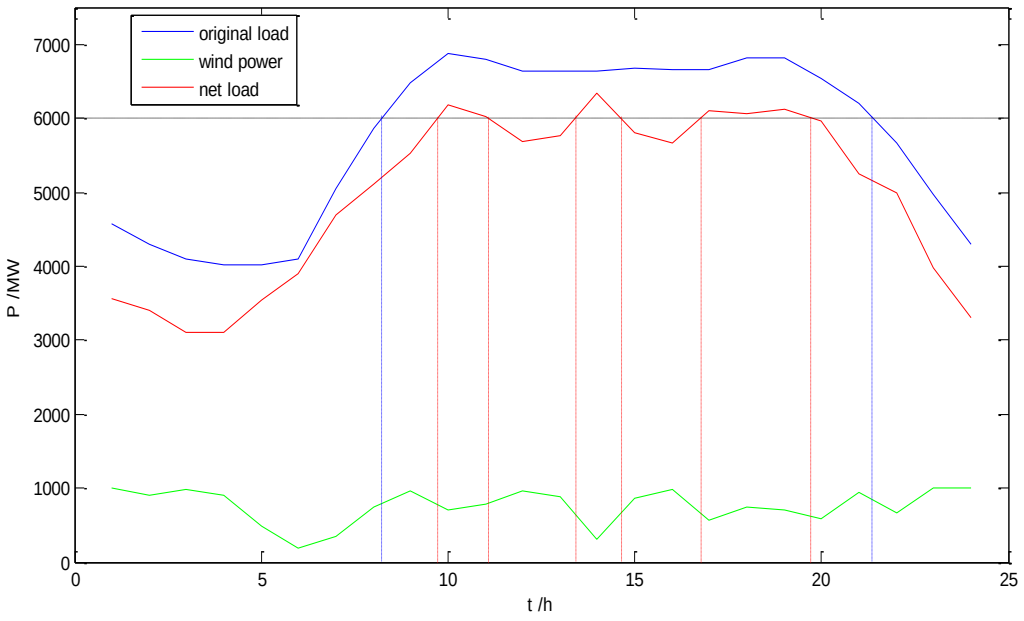

Fig. 2-6 The 24h original net load curve

After the access to wind power, not only the frequency of load fluctuations is increased, but also the interval of adjacent load transfer tends to decrease greatly. Once again, take the example of 6000MW load level as shown in Fig. 2-6. There exist totally three times of load upward transfers occurred in the net load curve, respectively, at 9:00, 13:00 and 16:00. Meanwhile, there are also three times of load downward transfers. Obviously, the interval between adjacent load transfers is quite small, where the smallest one is only 1 hour.

If it goes with one correspondence between the transfer frequency and unit operation, there would be three expected demands of unit startup and shutdown, respectively to be included in the evaluation of dynamic costs. However, if the generator has to be started up in a longer time interval, which means the operating limits or the down time limit is large, it is more likely to choose some time to maintain output state, rather than frequently start up or shut down. Relying merely on the frequency of the load fluctuations seems inadequate, more information is needed for calculation and evaluation.

For each load level, there exist two intervals between the upward transfer and its adjacent downward transfers, also two intervals between the downward transfer and it adjacent upward transfers. In actual operation, for the unit startup operation, only when both of these two intervals of upward transfer satisfy the time limits, i.e., the minimum up time and minimum down time, the request of unit startup can be fulfilled. Similarly, only when both of these two intervals of downward transfer satisfy the time limits, the request of unit shutdown can be fulfilled. For this reason, by recording each interval of load transfer, the load frequency curve is extended to the interval-frequency distribution series, which can both reflect the frequency information and distribution of timing information, more fully considering the timing characteristics of load fluctuation. Then the probabilistic production simulation method based on the equivalent interval frequency distribution is developed to give a more reasonable assessment of dynamic costs.

2.3 Load Interval Frequency Distribution Series

2.3.1 The Extension Principle

In order to obtain the time interval between each load transfer, for each load level k, while scanning the original load timing curve, not only it needs to cumulate load transfer frequency, but also every upward and downward transfer moment is recorded. Set the period between two

adjacent upward transfers as one time structure and calculate the inside two time intervals, respectively denoted as *m* and *n*, the item *m* represents the load upwards duration, *n* is the load downwards duration and their unit depends on the time step, usually it's recorded by hour. Meanwhile, set the period between two adjacent downward transfers as another time structure and calculate the two time intervals inside, respectively denoted as *n* and *m*, the item *m* can still represent the load upwards duration and *n* is the duration of the downward transfer as shown in Fig. 2-7. Thus, for the load level *k*, we can get two different time structures, and are counted as $a_{(k,m,n)}$ and $b_{(k,n,m)}$ Each time structure contains two time intervals, i.e., load upward transfer duration *m* and downward duration *n*. Time structure $a_{(k,m,n)}$ describes the downward transfer of load level *k* with which the adjacent front and back time interval is respectively *m* and *n*. According to the minimum up time and minimum down time of the corresponding unit, it can be used to determine the response of unit shutdown. While time structure $b_{(k,n,m)}$ describe the upward transfer of load level *k* with which the adjacent front and back time interval is respectively *n* and *m* to determine the demand of unit startup.

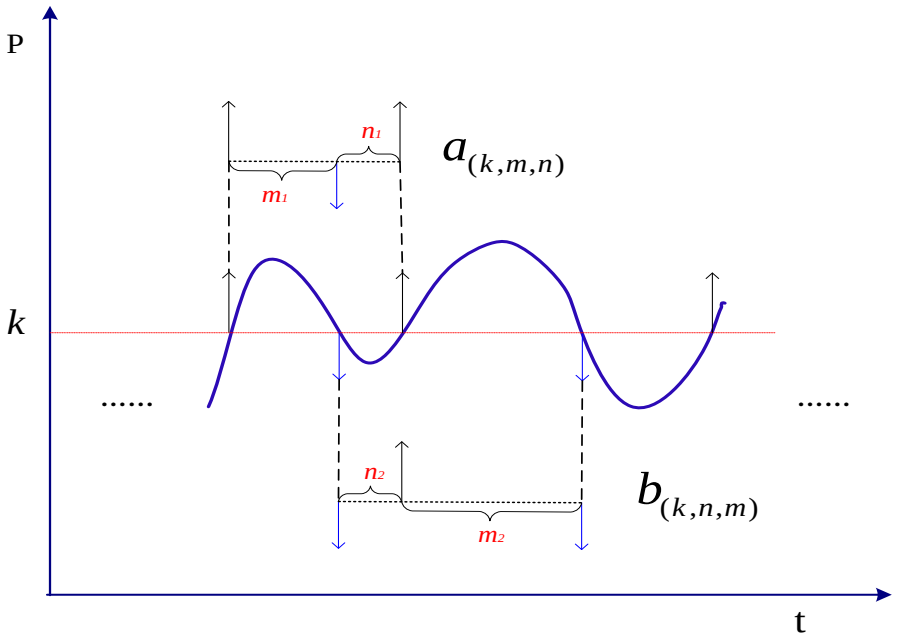

Fig. 2-7 The geometric explaination of time structure

For each load level, the frequency of load upward transfer within the study period is exactly equal to the one of downward transfer. Therefore, the total value of both time structure are the same and equal to the corresponding load frequency in the load frequency curve. In order to depict each time interval of load transfer simultaneously, we add these two time structure values, then divide by 2 so that the numerical value can be in accord with the load

frequency curve. Thus, the combined structure can be obtained and denoted as $IF(k)$ in this thesis to describe the interval-frequency distribution of load level *k*. In the discrete case, assuming that the time step is an integer value of 1 hour, load step size is an integer of 1 MW. At this moment, the interval-frequency distribution for load level *k* can be represented as follows:

$$IF(k)=\frac{1}{2}\left(\sum_{m=1}^{M}\sum_{n=1}^{N}a_{(k,m,n)}+\sum_{m=1}^{M}\sum_{n=1}^{N}b_{(k,n,m)}\right) \tag{2-4}$$

Where,

M——the maximum time interval of load upward duration;

N——the maximum time interval of load downward duration.

Element $a_{(k,m,n)}$ represents the downward transfer frequency of load level *k* with which the two adjacent time intervals are *m* and *n*, and the other element $b_{(k,n,m)}$ represents the upward transfer frequency of load level *k* with which the two adjacent time intervals are *n* and *m*. They are together to reflect the interval-frequency distribution for load level *k*. In the study period T, the last transfer is connected with the first one to make up another time structure. For the zero transfer load, i.e., the base load, the time structure can be expressed as $a_{(k,T,0)}=1$, or $b_{(k,0,T)}=1$ which means the load upward duration is the study period T. In addition, the following relationships are valid for all load levels, i.e., the sum of all the time intervals of time structures is just equal to the entire study period T.

$$\begin{aligned}&\sum_{m=1}^{M}\sum_{n=1}^{N}a_{(k,m,n)}=\sum_{n=1}^{N}\sum_{m=1}^{M}b_{(k,n,m)}=f_L(k)\\&\sum_{m=0}^{M}\sum_{n=0}^{N}(m+n)\times a_{(k,m,n)}=\sum_{n=0}^{N}\sum_{m=0}^{M}(n+m)\times b_{(k,n,m)}=T\end{aligned} \tag{2-5}$$

For all load levels within the study scope, the interval-frequency distribution can be formed, which corresponds to the frequency curve. The whole interval-frequency of distribution. can be expressed as two three-dimensional arrays:

$$\begin{aligned}A_{K\times M\times N}&=\left[a_{(k,m,n)}\right]_{K\times M\times N}\\B_{K\times N\times M}&=\left[b_{(k,n,m)}\right]_{K\times N\times M}\end{aligned} \tag{2-6}$$

Where:

K——is the discrete values of maximum system load.

Each element in the three-dimensional array represents one time structure. That is to say, $a_{(k,m,n)}$ is meaning the element of which three-dimensional parameters are *k*, *m*, and *n*. In order to visualize corresponding interval-frequency distribution for load level *k*, put the time structure into the spatial coordinate as shown in Fig. 2-8. The horizontal axis and the vertical axis in the bottom represents the load upward duration and downward duration, respectively. The vertical axis represents the corresponding frequency, i.e., the value of $a_{(k,m,n)}$ and $b_{(k,n,m)}$. A similar chart can be done for each load level *k*.

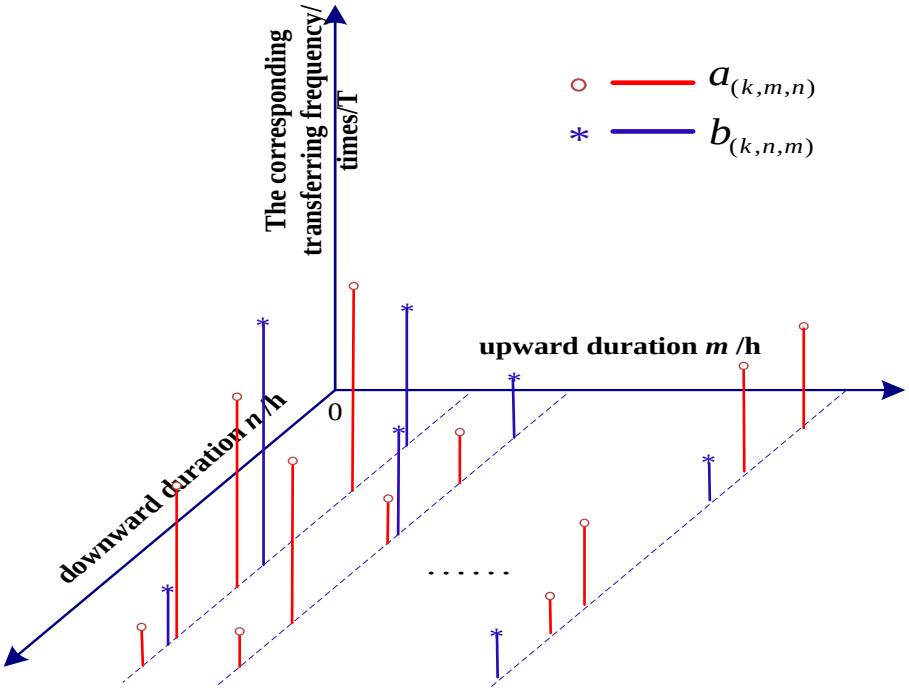

Fig. 2-8 The interval-frequency distribution of load level *k*

2.3.2 Simple Example Aanlysis

To further explain the extension principle of interval-frequency distribution series, this section illustrates one simple example of one week load (168 hours) for analysis where load step is taken as 50MW and discrete time value is 1h, the original load data shown in Fig. 2-9.

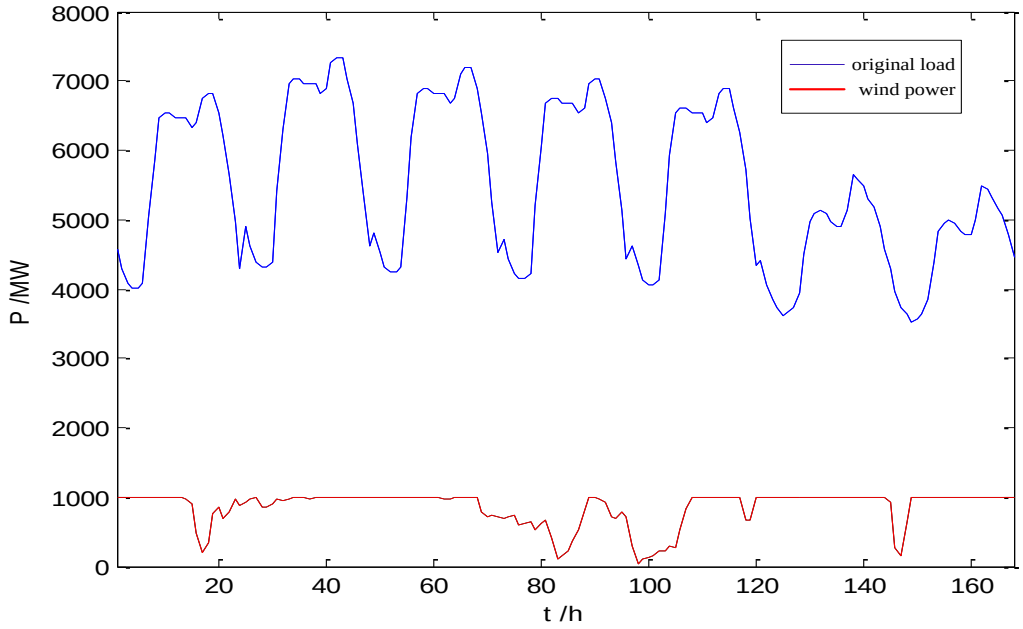

Fig. 2-9 The original load data of the simple example

Take the load level 4150MW for example, i.e., discrete value is 83. First of all record each upward and downward load transfer moment while scanning the original load curve. The results are as follows in Table 2-1. Then according to the downward transfer moment, the whole period can be divided into different time structures $a_{(k,m,n)}$ as shown in Fig. 2-10. Similarly, according to the upward transfer moment, we can get another different type of time structures $b_{(k,n,m)}$. After that, calculate all the time intervals in the time structure and we can clearly see the distribution information.

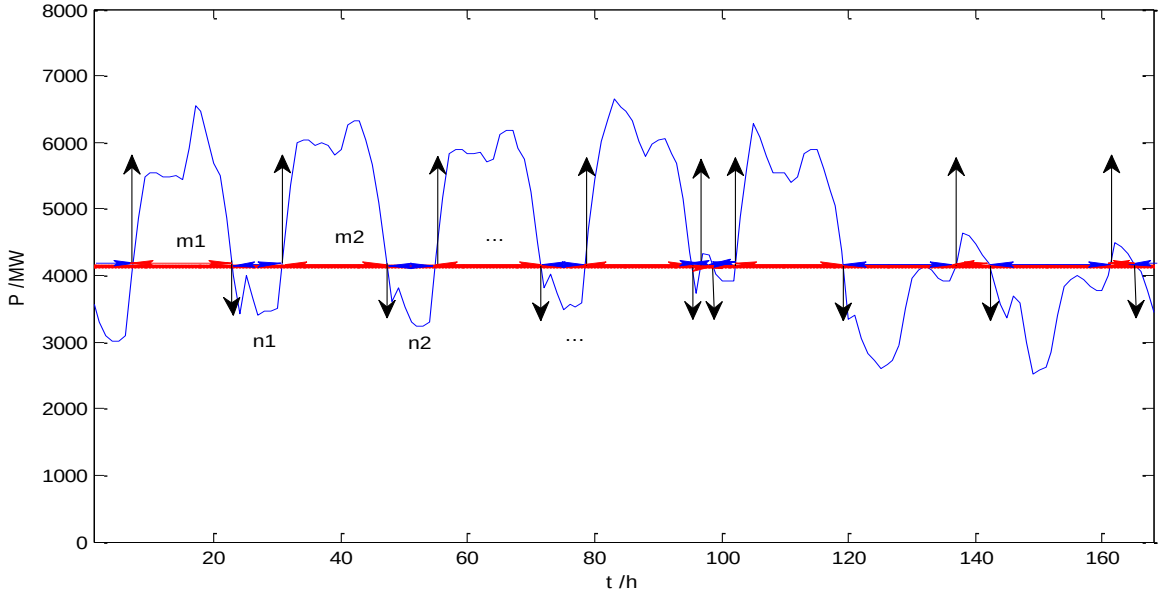

Fig. 2-10 The original chronological net load curve

Table 2-1 The transfer moment of load level 4150MW

i	1	2	3	4	5	6	7	8
i-th upward transfer moment	6	29	53	77	95	101	136	160
i-th downward transfer moment	21	46	70	94	97	118	141	164

Concluded from Table 2-1, there are totally 8 times of upward load transfers and 8 times of downward load transfers for load level 4150MW in the study time period. For the first type of time structure $a_{(k,m,n)}$, the whole period 168 hours are divided into 8 time structures based on the above theory. The last transfer is combined with the first one. Fig. 2-11 and Table 2-2 show the process of segmentation and calculation. Cumulate the sum of time structures which have the same of both time intervals. For example, there are two time structures of both which the upward duration is 17hrs and the downward duration is 7hrs. Hence the element $a_{(83,17,17)}$ is equal to 2. Among these time structures, we have two special time structures which have a quite small time interval, such as $a_{(83,2,4)}$ and $a_{(83,17,1)}$. If one unit loading level is exactly 4150MW, we can just take advantage of these time structures to determine the shutdown demand. Similarly, for the second kind of time structure, every adjacent downward transfer moment make up one time structure. The segmentation and calculation process is referred in Fig. 2-12 and Table 2-3.

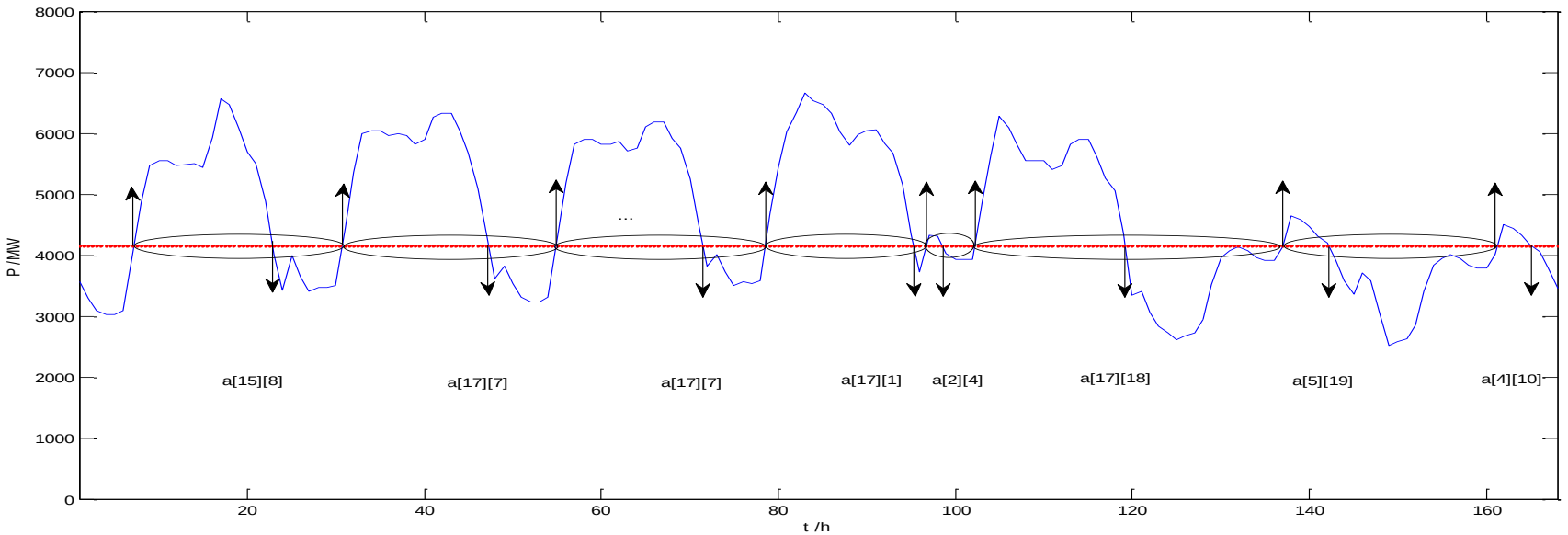

Fig. 2-11 The segmentation of first type of time structure $a_{(k,m,n)}$ for load level 4150MW

Table 2-2 The calculation of first type of time structure $a_{(k,m,n)}$ for load level 4150MW

i	**1**	**2**	**3**	**4**	**5**	**6**	**7**	**8**	
↑	6	2	5	7	9	10	13	16	6+16
		9	3	7	5	1	6	0	8
↓	21	46	70	94	97	118	114	164	
i-th $a_{(k,m,n)}$	$a_{(83,15,8)}$	$a_{(83,17,7)}$	$a_{(83,17,7)}$	$a_{(83,17,1)}$	$a_{(83,2,4)}$	$a_{(83,17,18)}$	$a_{(83,5,19)}$	$a_{(83,4,10)}$	

$a_{(83,2,4)}$ =1, $a_{(83,4,10)}$ =1, $a_{(83,5,19)}$ =1, $a_{(83,15,8)}$ =1, $a_{(83,17,1)}$ =1, $a_{(83,17,7)}$ =2, $a_{(83,17,18)}$ =1

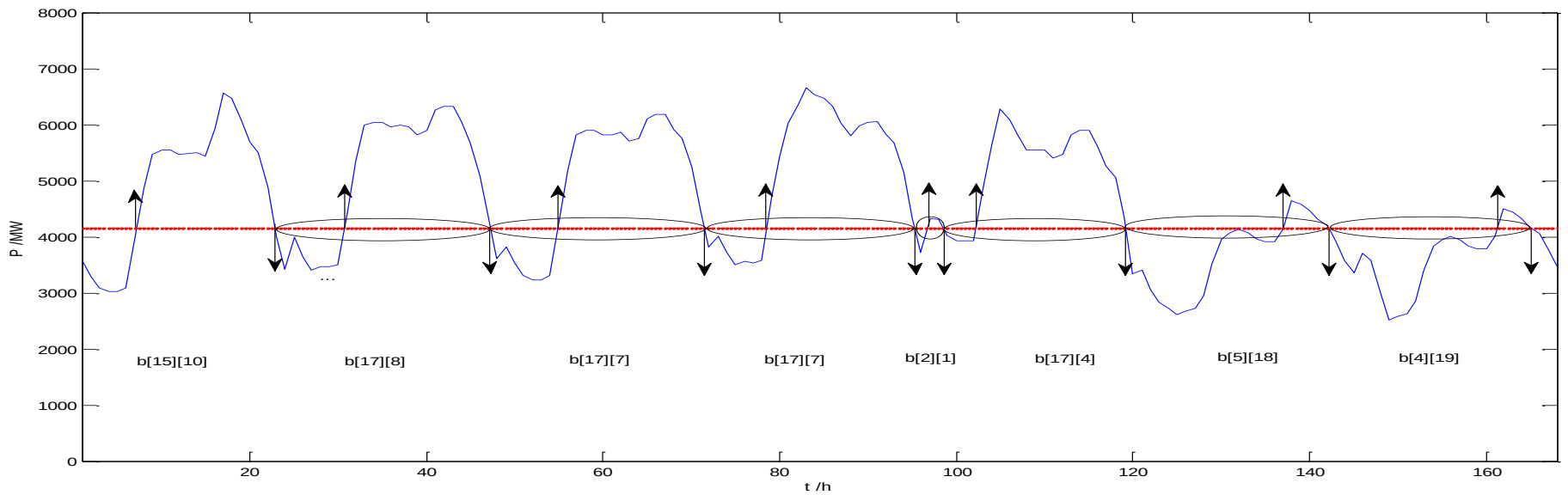

Fig. 2-12 The segmentation of second type of time structure $b_{(k,n,m)}$ for load level 4150MW

Table 2-3 The calculation of second type of time structure $b_{(k,n,m)}$ for load level 4150MW

i	**1**	**2**	**3**	**4**	**5**	**6**	**7**	**8**
↓	2 1	4 6	7 0	9 4	9 7	11 8	11 4	16 4	21+16 8
↑	6	29	53	77	95	101	136	160	6+168
i-th $b_{(k,n,m)}$	$b_{(83,8,17)}$	$b_{(83,7,17)}$	$b_{(83,7,17)}$	$b_{(83,1,2)}$	$b_{(83,4,17)}$	$b_{(83,18,5)}$	$b_{(83,19,4)}$	$b_{(83,10,15)}$	

$b_{(83,1,2)}=1$, $b_{(83,19,4)}=1$, $b_{(83,18,5)}=1$, $b_{(83,10,15)}=1$, $b_{(83,4,17)}=1$, $b_{(83,7,17)}=2$, $b_{(83,8,17)}=1$

Corresponding to the spatial coordinates, we can clearly see the distribution of each load transfer for the load level 5140MW as shown in Fig. 2-13. The time structure marked in red which means its corresponding time interval is a little small and it locates more close to the two axis in the bottom plane.

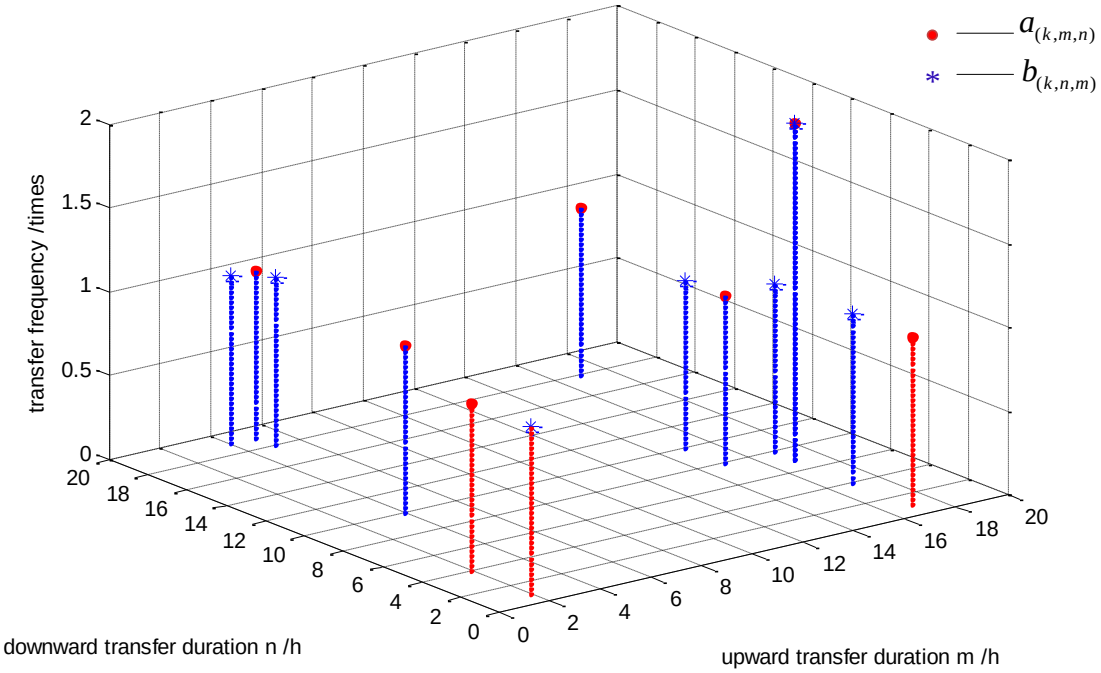

Fig. 2-13 The interval-frequency distribution of load level 4150MW

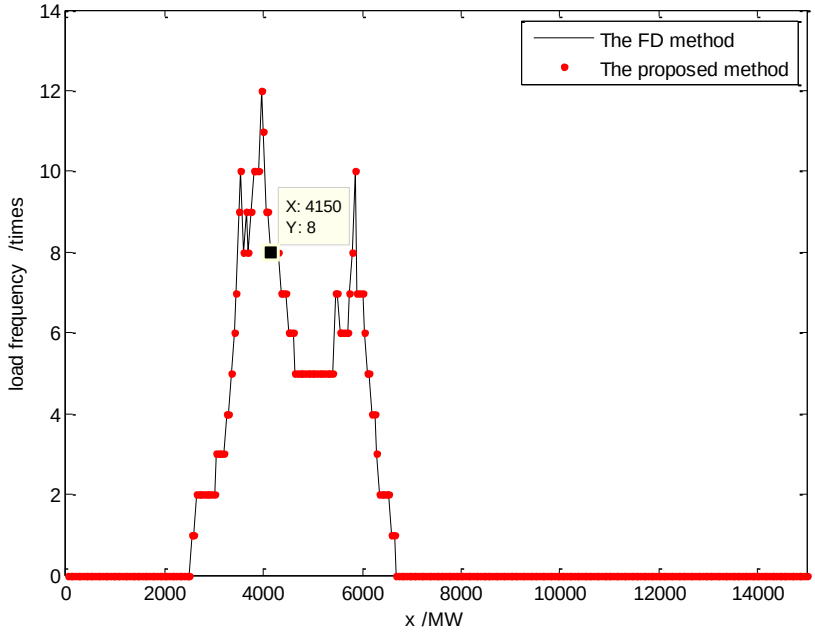

Fig. 2-14 The comparison of the original load frequency curves

Add the time interval in each time structure in Table 2-1 and multiply by the corresponding frequency, we can easily obtain that the value is just equal to 168 hours, which

is the exact study period. Furthermore, the frequency is also equal to 8 times for the load level 4150MW. Accordingly, the interval-frequency distribution for the other load levels can be restored into the load frequency curve according to the formula (2-6) as shown in Fig. 2-14. The curve in black is from the FD method and the red one is recovered in the proposed method. We can find that these two curve are fully consistent with each other, the transfer frequency for load level 4150MW is equal to eight times. This indicates that the interval-frequency distribution series can accurately restore to the load frequency curve, containing all the information of load frequency curve, and can reflect timing distribution of each load transfer through the adjacent time interval.

2.4 Brief Summary

Centered around how to describe the timing characteristic of the load, this chapter analyzes the shortcomings of the load duration curve and load frequency curves with simple illustrations respectively. To a certain degree both of them have limitations in terms of reflecting the timing fluctuation characteristics of the load. Then the load frequency curve is extended to the interval-frequency distribution based on load transfers. For each load level *k*, while scanning the original load timing curve, not only we need to accumulate the load transfer times but also to record every moment of each transfer is required. Set the adjacent upward transfer as one kind of time structure $a_{(k,m,n)}$, which is used to represent the downward transfer of which the front and back adjacent time interval is *m* and *n*. the item *m* means the upward transfer duration and *n* for the downward transfer duration. Similarly, set the adjacent downward transfer as another type of time structure $b_{(k,n,m)}$ to represent the upward transfer of which the front and back adjacent time interval is *n* and *m*. In the form of these two kinds of time structures, we can keep a record of the front and back adjacent time intervals of each load transfer to reflect the distribution of frequency information and timing fluctuations. Thereby a new probabilistic production simulation is developed based on this new interval-frequency distribution to get a more reasonable evaluation of unit startup and shutdown.

Also by a simple example, the interval-frequency distribution extension principle is further illustrated and compare it with the load frequency. We can conclude that in the interval-frequency distribution can be accurately restored into the load frequency curve and contain all the information of load frequency curve, reflecting timing distribution of each load transfer through the adjacent time interval.

3 Probabilistic Production Simulation Based on Equivalent Interval Frequency Distribution

The core of power system probabilistic production simulation algorithm is to consider both of the fluctuation of load and the forced outages of generating units. Just because of the consideration of these two factors, the whole process of power system generation can be deeply described to calculate the related reliability index of operation and the production cost, providing a strong scientific basis for the development of rational economic plan. Last chapter has introduced a new description of stochastic volatility load model based on the interval-frequency distribution. This chapter will first discuss the typical generator model, then the basic principle of the traditional probabilistic production simulation will be simply introduced. Meanwhile the Frequency and Duration method will also be explained to develop the proposed method: Power system probabilistic production simulation based on equivalent interval-frequency distribution. Finally it will evaluate the assessment of probabilistic production simulation, including the generator production, reliability index, the expected frequency of unit startup and shutdown, and the related dynamic cost.

3.1 Profile of Power System Probabilistic Production Simulation

Due to various technical reasons, the generator may be randomly forced into outages in its lifetime and then recovered into operation state by repair, working like a loop, as shown in Fig. 3-1.

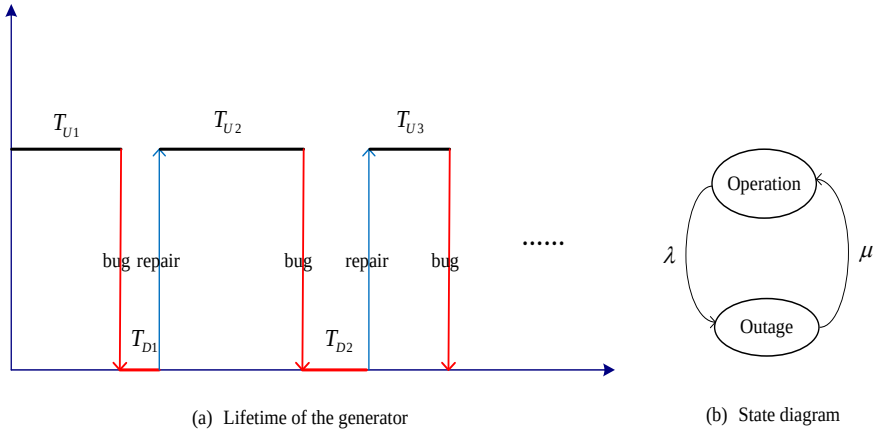

Fig. 3-1 The lifetime processes and state diagram of generator

In Fig. 3-1, the item of T_{U1}, $T_{U2},\cdots T_{Un}$ is the up time an T_{D1}, $T_{D2},\cdots T_{Dn}$ is the down time due to a fault outage, *n* is the total number of faults in its lifetime. According to the reference [19], three parameters can be defined which are closely related to the unit reliability. The Mean Time To Failure (MTTF) is the average time that the unit can run before a failure occurs, i.e., the length of time the unit is expected to last in operation. The higher the system reliability is, the longer MTTF will be. The Mean Time To Repair (MTTR) is the average time from the failure to recover in the middle of the period. The shorter MTTR represents a better recoverability. The last one is the Mean Time Between Failures (MTBF), which is the predicted elapsed time between inherent failures of units during operation. Undoubtedly, the longer MTBF means that it has a stronger the ability to work properly.

$$\begin{aligned} MTTF &= \frac{1}{n}\sum_{i=1}^{n} T_{Ui} \\ MTTR &= \frac{1}{n}\sum_{i=1}^{n} T_{Di} \\ MTBF &= MTTF + MTTR \end{aligned} \tag{3-1}$$

Thus, the probability of generator outage, i.e., the Forced Outage Rate (FOR) *q* can be obtained as follows.

$$q = \frac{MTTR}{MTBF} \tag{3-2}$$

The essence of conventional probabilistic production simulation is to transform the load curve into load duration curve and the effect of random outages of generating units is taken into account by increasing the system load to develop the effective load duration curve. It reflects that when a unit turns into a outage state with a certain probability, the other rest units will face a relatively larger equivalent load duration curve, which means to carry on more load [19]. There is a representative algorithm named Equivalent Energy Function method [20] [21], of which the computational accuracy and speed are outstanding. It first employs the discrete method to transform the original load duration curves $F(x)$ introduced last chapter into equivalent energy function $E(J)$. Dividing the abscissa into divisions of $F(x)$, the discrete energy function is defined as follows.

$$E(J) = \int_{x}^{x+\Delta x} F(x)dx \tag{3-3}$$

Where:

Δx ——the load step in the simulation process;

J—— $J =< x/\Delta x > +1$, an integer of not more than $x/\Delta x$.

The term $E(J)$ Is the electric energy which corresponds to the area of the interval $(x \quad x+\Delta x)$ under the load duration curve $F(x)$, namely the segment energy of this load level *x*. According to the well known convolution formula, combine the generator outages with load model together. Assumes that the corresponding energy function of original load duration curve is $E^{(0)}(J)$ and the effective one $E^{(i-1)}(J)$ is after loading the first *i-1* units. As shown in Fig. 3-2, let's arrange the *i-th* unit with capacity C_i and forced outage rate q_i, the corresponding equivalent energy function after convolution will be:

$$E^{(i)}(J) = p_i E^{(i-1)}(J) + q_i E^{(i-1)}(J - K_i) \tag{3-4}$$

Where:

K_i ——is the corresponding discrete values of *i-th* unit capacity, $K_i = C_i/\Delta x$.

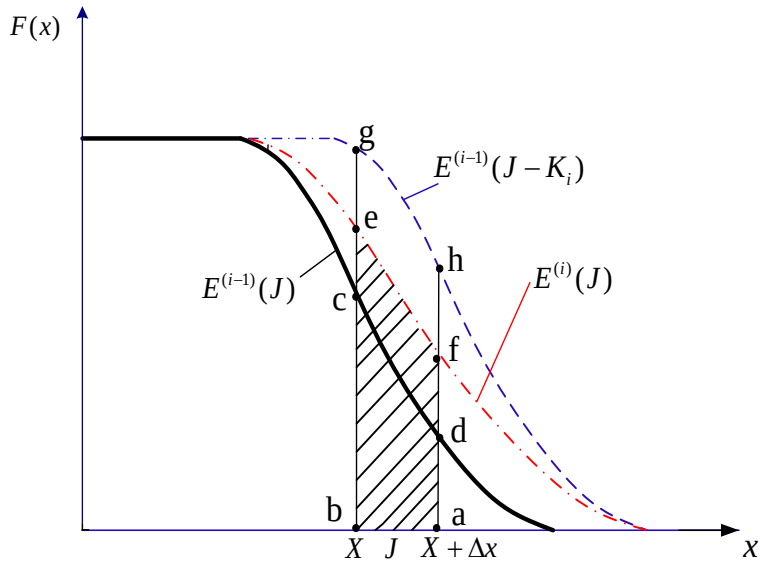

Fig. 3-2 The form of equivalent energy function

$E^{(i-1)}(J)$ and $E^{(i-1)}(J-K_i)$ correspond to the area *abcd* and *abgh* and abgh in Fig. 3-2, respectively. The shade area *abef* present $E^{(i)}(J)$. Δx should be selected as a common factor of all unit capacities, so that K_i can always be a integer.

Analog to the EEF method, the equivalent load frequency curve in the frequency and duration method is also obtained through standard convolution. The potential random failures

of unit is considered to add an equivalent part of load. Assume the equivalent load frequency curve after loading the first *i-1* units is $f_e^{(i-1)}(x)$ and the equivalent one after loading the *i-th* units is $f_e^{(i)}(x)$.

$$f_e^{(i)}(x) = p_i f_e^{(i-1)}(x) + q_i f_e^{(i-1)}(x - C_i) \tag{3-5}$$

Where:

q_i ——the forced outage rate of *i-th* unit;

p_i ——the normal operation probability of *i-th* unit, $p_i = 1 - q_i$;

C_i ——the capacity of *i-th* unit.

This part reflects the process that the initial load frequency curve is moved continuously right with the increased equivalent load, i.e., with the potentially random failure when leading each unit [38]. As shown in Fig. 3-3, the *x* axis is the equivalent system load. Just as the case that the coordinate is left shifted for correction in EEF method, the equivalent load frequency curve after convolution should be also needed to shift right in order to guarantee that each frequency has a one-to-one correspondence with system load. The item $p_i f_e^{(i-1)}(x)$ and $q_i f_e^{(i-1)}(x - C_i)$ in formula (3-5) respectively analog the shape components of normal operation and outage of *i-th* unit. They are together describing the shape variations of the equivalent load frequency curve $f_e^{(i)}(x)$ due to the potentially unit failure.

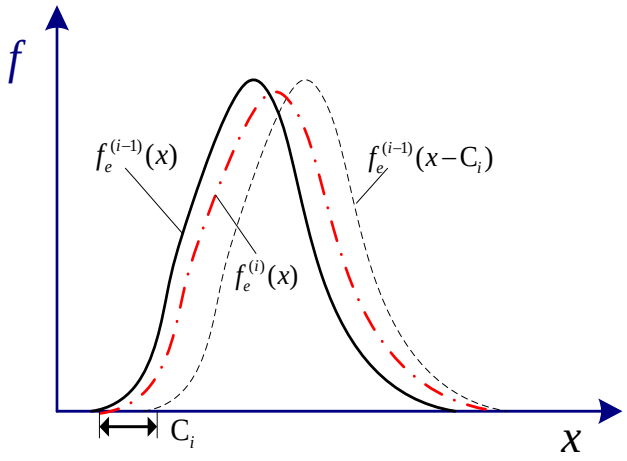

Fig. 3-3 The form of equivalent load frequency curve

At the same time, there exist some possibility that the unit unplanned shutdown and startup may occur because of the random failure of the *i-th* unit. The expected added times of load transfer can be calculated by dividing the whole up time by its mean time between

failures(MTBF).

$$N_{\mathrm{LT}}^{i}=\frac{F^{(i-1)}(x-C_i)-F^{(i-1)}(x)}{MTBF_i} \tag{3-6}$$

Where:

$MTBF_i$ ——the mean time between failures of *i-th* unit;

$F^{(i-1)}(x)$ ——the equivalent load duration curve after loading the first *i-1* units.

The numerator part $F^{(i-1)}(x-\mathrm{C}_i)-F^{(i-1)}(x)$ means the expected up time in the load level *x* of *i-th* unit. When combined with EEF method, the formula (3-6) can be expressed as follows.

$$N_{\mathrm{LT}}^{i}=\frac{E^{(i-1)}(k-K_i)-E^{(i-1)}(k)}{\tau_i\Delta x} \tag{3-7}$$

Where:

Δx ——the load step;

$E^{(i-1)}(k)$ ——the equivalent energy function after loading the first *i-1* units.

This part is the additional shutdown and startup due to the unit state recycle over the study period, directly reflecting the effect of the unit failure. However, since the unit' MTBF is usually quite large according to the IAEA database, the average parameter of modern units, is generally more than 2000 hours. So compared with the first part, this part contributes quite a little to the final calculation results and can be ignored [33].

In the evaluation system of FD method, the frequency of unit shutdown is equal to the one of unit startup, the expected times of *i-th* unit startup and shutdown in the study period T is calculated as follows:

$$F_i^{start}=F_i^{end}=Tp_i f_e^{(i-1)}(J_{i-1}) \tag{3-8}$$

Where:

J_{i-1}——the loading position of *i-th* unit, $J_{i-1}=\sum_{j=1}^{i-1}C_j \Big/ \Delta x$ 。

The FD method evaluates the assessment of dynamic costs through only part information of load fluctuations but it is not able to consider the feasibility of the unit startup and shutdown in short time interval, which will lead to a deviation in the result. With the increasing penetration of non-dispatchable technologies, such as the wind power, the system load fluctuates more significantly thus making this kind of error larger. In order to obtain a more rational evaluation results, we employ the interval-frequency distribution series extended last

chapter instead of load frequency curve, reflecting both the fluctuation frequency information and timing distribution to develop the new probabilistic simulation algorithms.

3.2 Probabilistic Production Simulation Based on Equivalent Interval Frequency Distribution

Also by standard convolution, the equivalent interval-frequency distribution is obtained, considering the influence of random unit failures as continually updating each time structure in the original interval-frequency distribution series. When the unit failure occurs, the equivalent system load will leap to a higher level, which will result in some additional load transfers. The second part $\frac{F^{(i-1)}(x-C_i)-F^{(i-1)}(x)}{\tau_i}$ is very small since the modern units are quite reliable, and will be neglected. In the assumption that the system has I units, the equivalent interval-frequency distribution series after arranging the first *i-1* units is $IF_e^{(i-1)}(k)$, and the one after loading the *i-th* unit is calculated as:

$$\begin{aligned} IF_e^{(i)}(k) &= p_i IF_e^{(i-1)}(k) + q_i IF_e^{(i-1)}(k-K_i) \\ &= \frac{1}{2}\sum_{m=0}^{M}\sum_{n=0}^{N}\left(p_i a_{(k,m,n)}^{i-1} + q_i a_{(k-K_i,m,n)}^{i-1} + p_i b_{(k,m,n)}^{i-1} + q_i b_{(k-K_i,m,n)}^{i-1} \right) \end{aligned} \tag{3-9}$$

Where:

q_i ——the forced outage rate of *i-th* unit;

p_i ——the normal operation probability of *i-th* unit being in service, $p_i = 1 - q_i$;

C_i ——the capacity of *i-th* unit;

K_i ——the corresponding discrete values of *i-th* unit capacity, $K_i = C_i / \Delta x$.

Table 3-1 The calculation process of *i-th* unit production simulation

k	*(i-1)-th* unit		*i-th* unit
	$a_{(k,m,n)}^{i-1}$	$a_{(k-K_i,m,n)}^{i-1}$	$a_{(k,m,n)}^{i}$
1	$a_{(1,m,n)}^{i-1}$	0	..
2	$a_{(2,m,n)}^{i-1}$	0	$p_i a_{(2,m,n)}^{i-1}$

Table 3-1(continued) The calculation process of *i-th* unit production simulation

k	*(i-1)-th* unit		*i-th* unit
	$a^{i-1}_{(k,m,n)}$	$a^{i-1}_{(k-K_i,m,n)}$	$a^{i}_{(k,m,n)}$
3	$a^{i-1}_{(3,m,n)}$	0	$p_i a^{i-1}_{(3,m,n)}$
⋮	⋮	⋮	⋮
K_i+1	$a^{i-1}_{(K_i+1,m,n)}$	$a^{i-1}_{(1,m,n)}$	$p_i a^{i-1}_{(K_i+1,m,n)} + q_i a^{i-1}_{(1,m,n)}$
K_i+2	$a^{i-1}_{(K_i+2,m,n)}$	$a^{i-1}_{(2,m,n)}$	$p_i a^{i-1}_{(K_i+2,m,n)} + q_i a^{i-1}_{(2,m,n)}$
K_i+3	$a^{i-1}_{(K_i+3,m,n)}$	$a^{i-1}_{(3,m,n)}$	$p_i a^{i-1}_{(K_i+3,m,n)} + q_i a^{i-1}_{(3,m,n)}$
⋮	⋮	⋮	⋮
k	$a^{i-1}_{(k,m,n)}$	$a^{i-1}_{(k,m,n)}$	$p_i a^{i-1}_{(k,m,n)} + q_i a^{i-1}_{(k,m,n)}$
$k+1$	$a^{i-1}_{(k+1,m,n)}$	$a^{i-1}_{(k+1-K_i,m,n)}$	$p_i a^{i-1}_{(k+1,m,n)} + q_i a^{i-1}_{(k+1-K_i,m,n)}$
$k+2$	$a^{i-1}_{(k+2,m,n)}$	$a^{i-1}_{(k+2-K_i,m,n)}$	$p_i a^{i-1}_{(k+2,m,n)} + q_i a^{i-1}_{(k+2-K_i,m,n)}$
⋮	⋮	⋮	⋮

k	*(i-1)-th* unit		*i-th* unit
	$b^{i-1}_{(k,m,n)}$	$b^{i-1}_{(k-K_i,m,n)}$	$b^{i}_{(k,m,n)}$
1	$b^{i-1}_{(1,n,m)}$	0	$p_i b^{i-1}_{(1,n,m)}$
2	$b^{i-1}_{(2,n,m)}$	0	$p_i b^{i-1}_{(2,n,m)}$
3	$b^{i-1}_{(3,n,m)}$	0	$p_i b^{i-1}_{(3,n,m)}$
⋮	⋮	⋮	⋮
K_i+1	$b^{i-1}_{(K_i+1,n,m)}$	$b^{i-1}_{(1,n,m)}$	$p_i b^{i-1}_{(K_i+1,n,m)} + q_i b^{i-1}_{(1,n,m)}$
K_i+2	$b^{i-1}_{(K_i+2,n,m)}$	$b^{i-1}_{(2,n,m)}$	$p_i b^{i-1}_{(K_i+2,n,m)} + q_i b^{i-1}_{(2,n,m)}$

Table 3-1 (continued) The calculation process of *i-th* unit production simulation

k	*(i-1)-th* unit		*i-th* unit
	$b^{i-1}_{(k,m,n)}$	$b^{i-1}_{(k-K_i,m,n)}$	$b^{i}_{(k,m,n)}$
K_i+3	$b^{i-1}_{(K_i+3,n,m)}$	$b^{i-1}_{(3,n,m)}$	$p_i b^{i-1}_{(K_i+3,n,m)} + q_i b^{i-1}_{(3,n,m)}$
$\vdots$	$\vdots$	$\vdots$	$\vdots$
k	$b^{i-1}_{(k,n,m)}$	$b^{i-1}_{(k,n,m)}$	$p_i b^{i-1}_{(k,n,m)} + q_i b^{i-1}_{(k,n,m)}$
$k+1$	$b^{i-1}_{(k+1,n,m)}$	$b^{i-1}_{(k+1-K_i,n,m)}$	$p_i b^{i-1}_{(k+1,n,m)} + q_i b^{i-1}_{(k+1-K_i,n,m)}$
$k+2$	$b^{i-1}_{(k+2,n,m)}$	$b^{i-1}_{(k+2-K_i,n,m)}$	$p_i b^{i-1}_{(k+2,n,m)} + q_i b^{i-1}_{(k+2-K_i,n,m)}$
$\vdots$	$\vdots$	$\vdots$	$\vdots$

As shown in Table 3-1, in the convolution process, only the same type of time structures which also have the same two time intervals, i.e., the same value of *m* and *n*, can be multiplied by each other for convolution. After loading the *i-th* unit, the new time structure for load level *k*, contains the previous all-time structure information of both load level $k-K_i$ and load level of *k*. As Table 3-1 shows, the time structure is corrected, not only reflecting that the corresponding frequency of former time structure $[1 \quad K_i]$ is changed through multiplying by the normal operation probability of *i-th* unit for the load level, but also embodying that some new time structures will be formed in the other load level, such as the case that the load level $k+K_i$ will contain the time structure information of load level *k*. Similarly, restoring the corrected time structures into by the formula (2-6), the obtained equivalent interval-frequency distribution series can be recovered into its corresponding equivalent frequency load curve, comparing the equation (3-9) and formula (3-5), the following equation is still satisfied.

$$\begin{aligned} &\sum_{m=1}^{M}\sum_{n=1}^{N} a^{i}_{(k,m,n)} = \sum_{n=1}^{N}\sum_{m=1}^{M} b^{i}_{(k,n,m)} = f_e^{(i)}(k) \\ &\sum_{m=0}^{T}\sum_{n=0}^{T} (m+n)\times a^{i}_{(k,m,n)} = \sum_{n=0}^{T}\sum_{m=0}^{T} (n+m)\times b^{i}_{(k,n,m)} = T \end{aligned} \tag{3-10}$$

Based on the detailed information of time intervals in the corrected time structures, we

can expand the following production simulation evaluation.

3.3 Assessment Model of Probabilistic Production Simulation

3.3.1 Generator Production and Reliability Index

As for the expected energy calculation of each unit, we first define a discrete energy function based on the interval-frequency distribution series. As shown in Fig. 3-4, the energy of load level is equal to the sum of energy in each corresponding time structure. The energy of time structure can be obtain by multiplying the upward load transfer duration and the load step as shown by the shaded area in Fig. 3-4. Therefore the energy of load level k is calculated by the following formula.

$$E(k)=\sum_{m=1}^{M}\sum_{n=1}^{N}\Delta x\times m\times a_{(k,m,n)} \quad or \quad E(k)=\sum_{n=1}^{N}\sum_{m=1}^{M}\Delta x\times m\times b_{(k,n,m)} \tag{3-11}$$

Where:

Δx ——the load step in the simulation process;

m——the upward duration in each time structure.

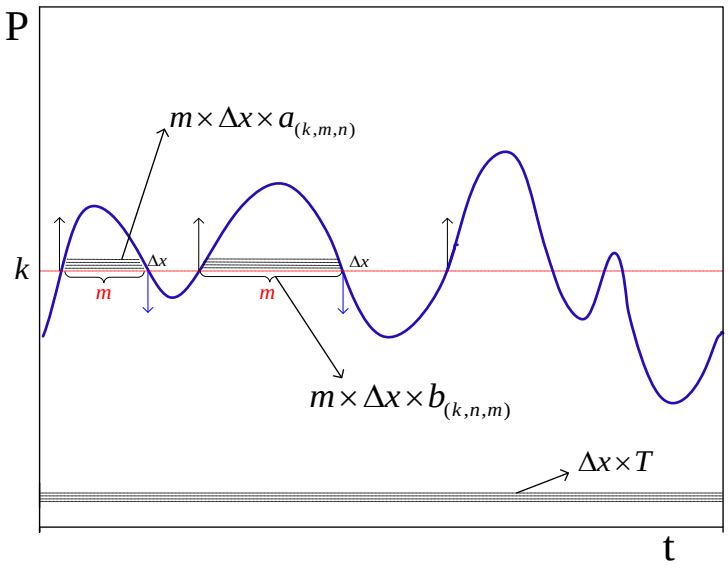

Fig. 3-4 The explaination of discrete energy function

Note that for the base load, the corresponding time structure $a_{(k,\mathrm{T},0)}=1$, so its energy is $E(k)=\Delta x\times T$. In this thesis, we just uniformly resort to the first type of time structure $a_{(k,m,n)}$.

Therefore, the total energy of system load can be expressed as:

$$E_D = \sum_{k=1}^{K}\sum_{m=0}^{T}\sum_{n=0}^{N} \Delta x \times m \times a_{(k,m,n)} \tag{3-12}$$

Where:

K——the corresponding discrete values of maximum load in the initial system.

As we all know, the desirable energy of power generator E_{gi} is decided by its corresponding loading interval, and the *i-th* generating unit should depend on the equivalent interval-frequency distribution $A^{i-1}_{K\times M\times N} = \left[a^{i-1}_{(k,m,n)} \right]_{K\times M\times N}$ just after loading the previous *i-1* units. The loading position for *i-th* unit, is exactly located at the whole capacity of first *i-1* installed units, i.e., the load level $J_{i-1} = \sum_{j=1}^{i-1} C_j \Big/ \Delta x$, and its loading interval is $[J_{i-1} \quad J_i]$ as shown in Fig. 3-5. Therefore add all the energy of time structures among $[J_{i-1} \quad J_i]$, and multiply by the normal operation probability p_i of *i-th* unit. We can get the expected energy for *i-th* unit production.

$$E_{gi} = p_i \sum_{k=J_{i-1}}^{J_i}\sum_{m=1}^{M}\sum_{n=1}^{N} \Delta x \times m \times a^{i-1}_{(k,m,n)} \tag{3-13}$$

Where:

J_{i-1}——the loading position for *i-th* unit, $J_{i-1} = \sum_{j=1}^{i-1} C_j \Big/ \Delta x$.

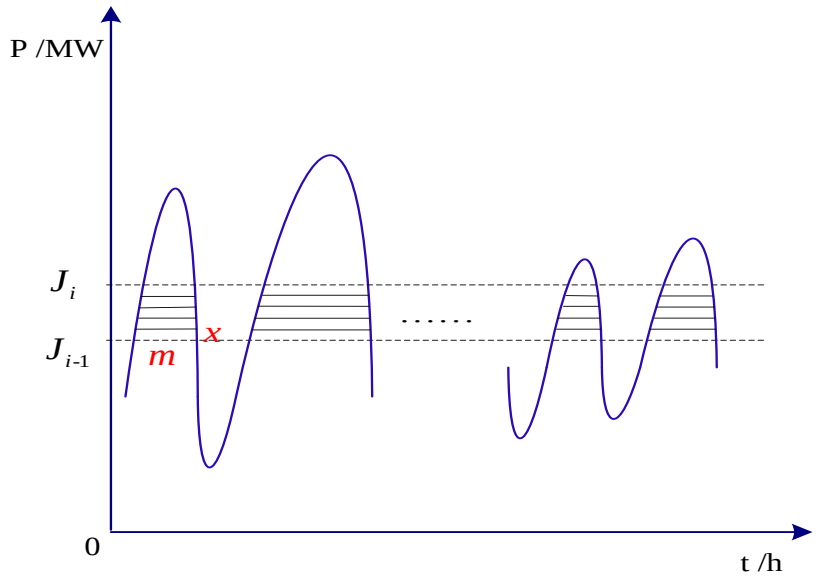

Fig. 3-5 The geometric interpretation for *i-th* unit expected energy calculation

Also by definition, we can deduce the formula to calculate the expected energy not served (EENS) and loss of load probability (LOLP). After loading all units, the unloaded interval is just $[J_I \quad J_I + K]$. Therefore, the equivalent time structure $a^I_{(k,m,n)}$ of the interval-frequency distribution can be employed to obtain EENS. As for LOLP, it means the loss of load probability after installing all units. We can just multiply the upward transfer duration *m* in the load level J_I by its transfer frequency in the equivalent time structure $a^I_{(J_I,m,n)}$, then divide by the study period T.

$$\begin{aligned} EENS &= p_i \sum_{k=J_I}^{J_I+K} \sum_{m=1}^{M} \sum_{n=1}^{N} \Delta x \times m \times a^I_{(k,m,n)} \\ LOLP &= \frac{1}{T} \sum_{m=1}^{M} \sum_{n=1}^{N} m \times a^I_{(J_I,m,n)} \end{aligned} \tag{3-14}$$

Where:

I——the total number of units;

J_I——the discrete value of total installed capacity, $J_I = \sum_{j=1}^{I} C_j \Big/ \Delta x$.

For the expected energy not served, we can subtract the total energy generated from the whole original system load.

$$EENS = E_D - \sum_{i=1}^{I} E_{gi} \tag{3-15}$$

3.3.2 Generator Expected Startup Frequency

Load transfer may reflect the demands of the generator startup and shutdown operation to some extent. But since the actual operation of the generator is determined by a variety of factors, such as the state of generator, the minimum up time and minimum down time, scheduling model and other common influence, which is a relatively complex decision results. It is difficult to get a accurate result only by the number of load transfer for the frequency of unit startup and shutdown. Accordingly, this thesis only presents an overall evaluation, which is close to the actual situation as much as possible.

Due to the minimum up time limit and minimum down time limit, if the duration when the system load is lower than the loading level is less than the minimum down time, the corresponding generator will probably decrease its output, or keep standby state, not just

require to shut down. Similarly, if the duration when the system load is higher than the loading level is less than the minimum up time, some other hot standby power will make up for these and the corresponding generator does not to start up. On the other hand, when the system load is greater than the loading load level for a long period, we can determine that its corresponding generator is at running state, and when the system load is less than the loading load level for a long period, the unit should be in the outage state. Dealing with time structures $a_{(k,m,n)}$ units are assumed to shutdown only when the front (*m*) and back (*n*) time intervals of the corresponding load level satisfy the minimum running time limit and minimum outage time limit, i.e., $m \geq m_{\min}^{i}$ and $n \geq n_{\min}^{i}$. At this point, we need to use the timing information of first type of time structure $a_{(k,m,n)}$, only when the downward duration *n* is greater than the minimum down time limit $n_{\min}^{i}$, and the upward duration *m* is greater than the minimum up time limit $m_{\min}^{i}$, can this downward transfer respond to shut down the unit. As shown in the Fig. 3-6, for the first case (a) of short-term fluctuation, it happens in a short interval, which can be totally neglected, the unit can adjust its output to keep balanced. In the case (b), before the load transfers downward, the corresponding unit should stay in the running state and afterwards, there happens the load transfer with a short interval of downward duration, this unit shutdown will not be demanded. In the case (c), before the load downward transfer, there is only a short upward duration, the unit itself is likely to be in the state of outage, so this situation is still not considered. Only in the last case (d), time intervals in the time structure are meeting the requirements, i.e. $m \geq m_{\min}^{i}$ and $n \geq n_{\min}^{i}$.

Similarly, for the unit startup operation, only when the front (*n*) and back (*m*) time intervals of the corresponding load level downward transfer satisfy the minimum down time limit and minimum up time limit, respectively, can this startup request be fulfilled. That is to mean, the second type of time structure $b_{(k,n,m)}$, only when the downward duration *n* is greater than the minimum down time limit $n_{\min}^{i}$, and the upward duration *m* is greater than the minimum up time limit $m_{\min}^{i}$, can this upward transfer be counted to start up the unit.

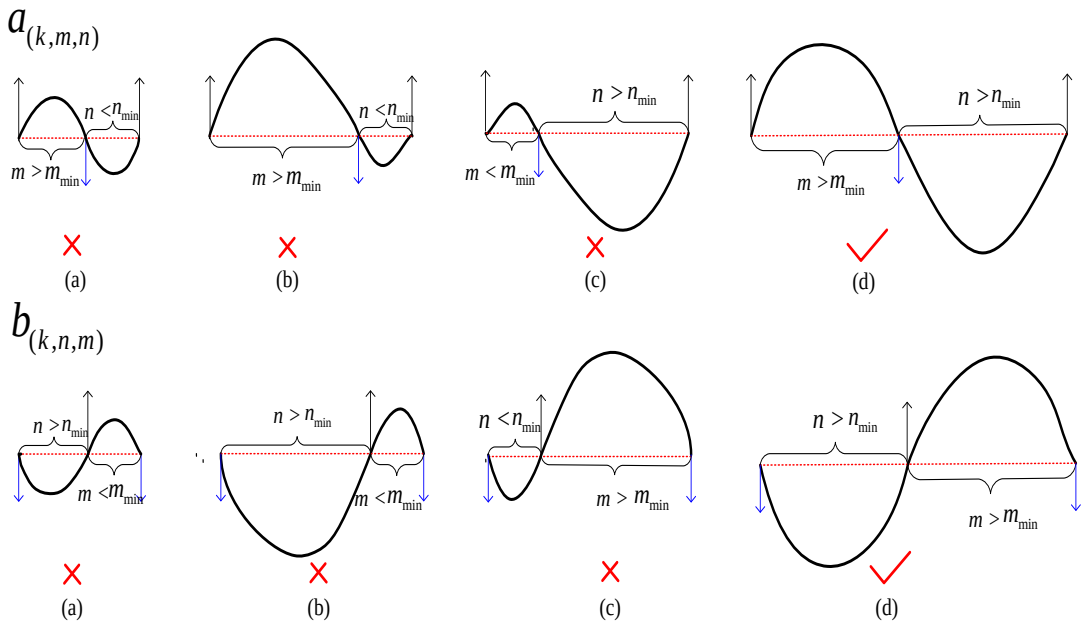

Fig. 3-6 The time structure to analyse the startup and shutdown response

According to the above strategy, the time structure is selected to meet the requirements and calculate the expected shutdown and startup frequency. Within the study period T, the total expected times of *i-th* unit startup and shutdown is determined by the equivalent interval-frequency distribution $A^{i-1}_{K\times M\times N}=\left[a^{i-1}_{(k,m,n)}\right]_{K\times M\times N}$ and $B^{i-1}_{K\times N\times M}=\left[b^{i-1}_{(k,n,m)}\right]_{K\times N\times M}$ after arranging previous *i-1* units. It goes as follows for the frequency of *i-th* unit.

$$F_i^{start}=p_i\sum_{m=m^i_{\min}}^{M}\sum_{n=n^i_{\min}}^{N}b^{i-1}_{(J_{i-1},n,m)}$$
$$F_i^{end}=p_i\sum_{n=n^i_{\min}}^{N}\sum_{m=m^i_{\min}}^{M}a^{i-1}_{(J_{i-1},m,n)} \tag{3-16}$$

Where:

$m^i_{\min}$——the minimum up time of *i-th* unit;

$n^i_{\min}$——the minimum down time of *i-th* unit;

J_{i-1}——the loading position of *i-th* unit.

For base load, the startup and shutdown frequency of units who take charge for this part of loads is equal to 0, since there is no load fluctuation at all. To give a comprehensive evaluation of the conventional generating unit startup and shutdown frequency, the Frequency of Generator Startup and Shutdown of Unit Capacity (FGSUC) I_{FGSUC}, is adopted to reflect the frequency of the operation per unit capacity. In other words, multiply the frequency of each

unit by its capacity, sum up together, and divide by the whole installed capacity. The equation is as follows.

$$I_{FGSUC} = \frac{\frac{1}{T}\sum_{i=1}^{I} C_i \left(F_i^{start} + F_i^{end} \right)}{\sum_{i=1}^{n} C_i} \tag{3-17}$$

So the corresponding startup and shutdown frequency of the removed time structure are as follows:

$$\begin{aligned} T_i^{start} &= p_i \sum_{m=1}^{M}\sum_{n=1}^{N} b_{J_{i-1}mn}^{i-1} - F_i^{start} \\ &= p_i \Big(\sum_{m=1}^{m_{\min}^i - 1}\sum_{n=1}^{N} a_{(J_{i-1},m,n)}^{i-1} + \sum_{m=1}^{M}\sum_{n=1}^{n_{\min}^i - 1} a_{(J_{i-1},m,n)}^{i-1} + \sum_{m=1}^{m_{\min}^i - 1}\sum_{n=1}^{n_{\min}^i - 1} a_{(J_{i-1},m,n)}^{i-1} \Big) \\ T_i^{end} &= p_i \sum_{n=1}^{N}\sum_{m=1}^{M} a_{J_{i-1}mn}^{i-1} - F_i^{end} \\ &= p_i \Big(\sum_{n=1}^{n_{\min}^i - 1}\sum_{m=1}^{M} b_{(J_{i-1},n,m)}^{i-1} + \sum_{n=1}^{N}\sum_{m=1}^{m_{\min}^i - 1} b_{(J_{i-1},n,m)}^{i-1} + \sum_{n=1}^{n_{\min}^i - 1}\sum_{m=1}^{m_{\min}^i - 1} b_{(J_{i-1},n,m)}^{i-1} \Big) \end{aligned} \tag{3-18}$$

Eliminating these time structures of short interval, will result in the factor that it needs to keep some units in the state of standby, which will make an economic effect to some extent. Here the Short Time Interval Proportion of Unit Capacity (STIPUC) I_{STIPUC} is induced to reflect this part influence from the point of view of the proportion of the total time.

$$I_{\mathrm{STIPUC}} = \frac{\frac{1}{T}\sum_{i=1}^{I} C_i \left(T_i^{start} + T_i^{end} \right)}{\sum_{i=1}^{n} C_i} \tag{3-19}$$

3.3.3 Dynamic Costs

The unit shutdown and startup operation results in the dynamic cost and it plays an important role in whole production cost, especially in the power system with wind power. So it is a key consideration in this thesis. According to Reference [33]-[38], dynamic cost of the conventional units usually includes the boiler startup costs, the turbine startup costs and the unit shutdown costs of downtime, specifically calculated as follows:

$$C_d = C_{\mathrm{TSU}} + C_{\mathrm{BSU}} + C_{sd} \tag{3-20}$$

Where:

C_{TSU} ——the turbine startup costs;

C_{BSU} ——the boiler startup costs;

C_{sd} ——the unit shutdown costs.

The process of turbine startup is to enhance the internal pressure to the rated one. In the different startup conditions, such as the case that the generator is set as a cold or hot standby, the cost of the turbine startup C_{TSU} is relatively fixed, only determined by the expected startup frequency [33]. Therefore, the turbine startup costs of *i-th* unit can be calculated as follows:

$$C_{\mathrm{TSU}} = \sum_{i=1}^{I} p_i C_i c_{\mathrm{TSU}}^{i} F_i^{\mathrm{start}} \tag{3-21}$$

Where:

c_{TSU}^{i} ——the single turbine startup cost of *i-th* unit.

As for the boiler startup process is to raise the temperature inside unit boiler the operating temperature and the startup costs C_{BSU} is dependent a lot on the time for which units have been offline T_{i_off}. If the unit is allowed to cool after off-loading, the heat will decay approximately exponentially with a known time constant. This is the continuous form of an equation given by Stirling. The longer the offline time is, the lower the operating temperature will be, and the higher the cost for boiler startup. Consequently, only the time structure $b_{(J_{i-1},n,m)}^{i-1}$ that meets the requirements can be taken into the account. As for the offline time, it is represented by the duration of the load downward transfer duration *n* instead of the average value in FD method, which also can improve the accuracy of the assessment, further close to the actual situation. The cost of bringing it to operating temperature will then be:

$$C_{\mathrm{BSU}} = \sum_{i=1}^{I} \sum_{m=m_{\min}^{i}}^{M} \sum_{n=n_{\min}^{i}}^{N} p_i C_i c_{\mathrm{BSU}}^{i} (1 - e^{-n/\tau_i^b}) b_{(J_{i-1},n,m)}^{i-1} \tag{3-22}$$

Where:

c_{BSU}^{i} ——the single boiler startup costs of *i-th* unit;

τ_i^b ——the boiler cooling time constant of *i-th* unit.

In the study period, the unit shutdown costs are relatively fixed, just depending on the unit shutdown frequency. So the total unit shutdown costs can be calculated by the following

formula.

$$C_{sd} = \sum_{i=1}^{I} p_i C_i c_{sd}^i F_i^{\text{end}} \tag{3-23}$$

Where:

C_{sd} ——the single unit shutdown costs of *i-th* unit.

In order to evaluate the impact of short term fluctuations in the time structure, the Short Time Interval Dynamic Cost (STIDC) I_{STIDC} is defined and calculated as follows.

$$I_{\text{STIDC}} = \frac{C_d{}' - C_d}{C_d{}'} \tag{3-24}$$

The item $C_d{}'$ is the dynamic costs, considering all the time structure when assessing the unit shutdown and startup frequency, i.e., its corresponding frequency is $F_i^{start\,'} = p_i \sum_{m=1}^{M}\sum_{n=1}^{N} b_{(J_{i-1},n,m)}^{i-1}$ and $F_i^{end\,'} = p_i \sum_{n=1}^{N}\sum_{m=1}^{M} a_{(J_{i-1},m,n)}^{i-1}$. I_{STIDC} can approximately reflect the proportion of dynamic costs caused by the short intervals in the total costs.

Based on the above dynamic cost analysis, we can carry out a comprehensive production cost for power generation, which includes the fuel of units, dynamic costs, environmental costs, and the customer interruption cost.

$$C_{total} = C_{fuel} + C_{envi} + C_{voll} + C_d \tag{3-25}$$

Where:

C_{fuel} ——the unit fuel cost;

C_{envi} ——the environmental costs;

C_{voll} ——the customer interruption cost.

Among them, the fuel costs and environmental costs depend on the electricity that the generator produce. The customer interruption cost is proportional to EENS. What's more, the preventable costs of wind power can be obtained as follows.

$$\Delta C = C_0 - C_1 \tag{3-26}$$

Where:

C_0 ——the total production costs excluding wind power;

C_1 ——the total production costs including wind power.

3.4 Calculating Flow of Probabilistic Production Simulation

The flow chart of probabilistic Production Simulation based on equivalent interval-frequency distribution is shown in Fig. 3-7.

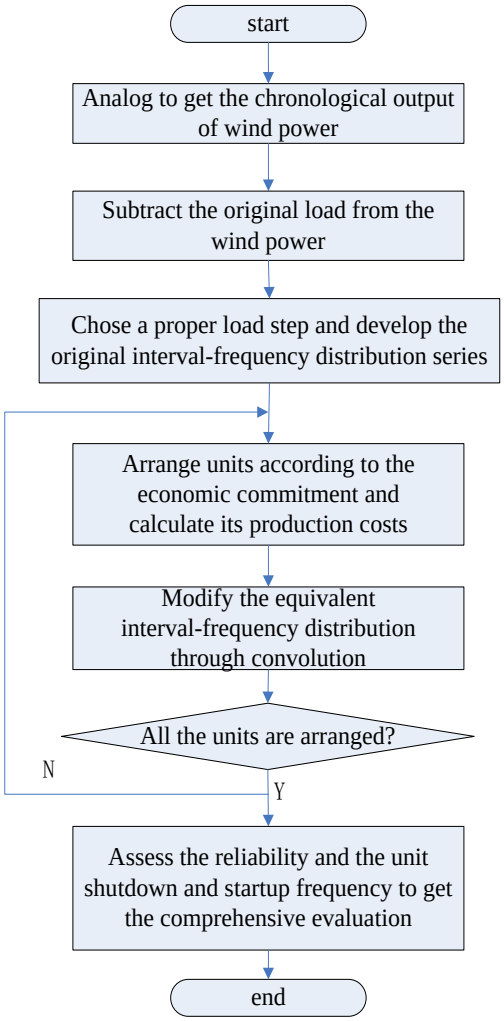

Fig. 3-7 Flow chart of the probabilistic production simulation

3.5 Brief Summary

This chapter focuses primarily on the fundamental principle of the proposed method based on the equivalent interval-frequency distribution, which is obtained by standard convolution, considering the random outage of unit as the modification of each time structure in the initial interval-frequency distribution. During the convolution process, only the time structures sharing both the same two adjacent time intervals, i.e., the same value of *m* and *n*, can be multiplied by convolution. In details, when getting the equivalent distribution after loading *i-th* unit, the new distribution compose both of the components of normal operation

$p_i a^{i-1}_{(k,m,n)} + p_i b^{i-1}_{(k,m,n)}$ and outage $q_i a^{i-1}_{(k-K_i,m,n)} + q_i b^{i-1}_{(k-K_i,m,n)}$ of i-th unit in the previous one. They are together describing the shape variations of the equivalent load frequency curve due to the potentially unit failure.

For expected generating energy calculation and reliability analysis, first define the energy function $E(k) = \sum_{m=1}^{M} \sum_{n=1}^{N} \Delta x \times m \times a_{(k,m,n)}$ based on the time structures $a_{(k,m,n)}$ of interval-frequency distribution, which means that the corresponding energy for each load is obtained by multiplying the load step with each upward duration. When all the units are committed, the unloaded load range is $[J_I \quad J_I + K]$, so we can employ the equivalent interval-frequency distribution $a^{I}_{(k,m,n)}$ to calculate the EENS. For the loss of load probability, which refers to the ratio of total downward durations on that specific load level J_I and the study period T. In short, the time structure is fully explored to evaluate the expected energy for each unit and reliability index.

As for the frequency of unit startup and shutdown, it is assumed that only when the corresponding adjacent two time intervals of the corresponding loading level are both meeting the minimum up time and down time limits, i.e., $m \geq m^{i}_{\min}$ and $n \geq n^{i}_{\min}$, can this load upward transfer respond the unit to start up. While only when the corresponding adjacent two time intervals of the corresponding loading level are both meeting the minimum time limits, i.e., $n \geq n^{i}_{\min}$ and $m \geq m^{i}_{\min}$, can this load downward transfer respond the unit to shut down. In this way, we can obtain a more reasonable assessment of the unit startup and shutdown frequency and the related dynamic cost, which is relatively more close to the actual situation.

4 Case Studies

This chapter analyze one numerical example, composed by the EPRI-36 generator system and IEEE RTS load data. According to the above theoretical models, this system is stochastically simulated based on the equivalent interval-frequency distribution series. And in order to verify the effectiveness and accuracy of this method, we will compare the results with the other conventional methods, such as compare the expected energy of each unit and reliability index with the one through Equivalent Energy Function method, and the dynamic costs with the one through Frequency and Duration method.

4.1 Basic Data

4.1.1 Load Data

The load data is referring to IEEE RTS load data [42] and the study period is one month, i.e., 30 days (720 hours), as shown in Fig. 4-1.

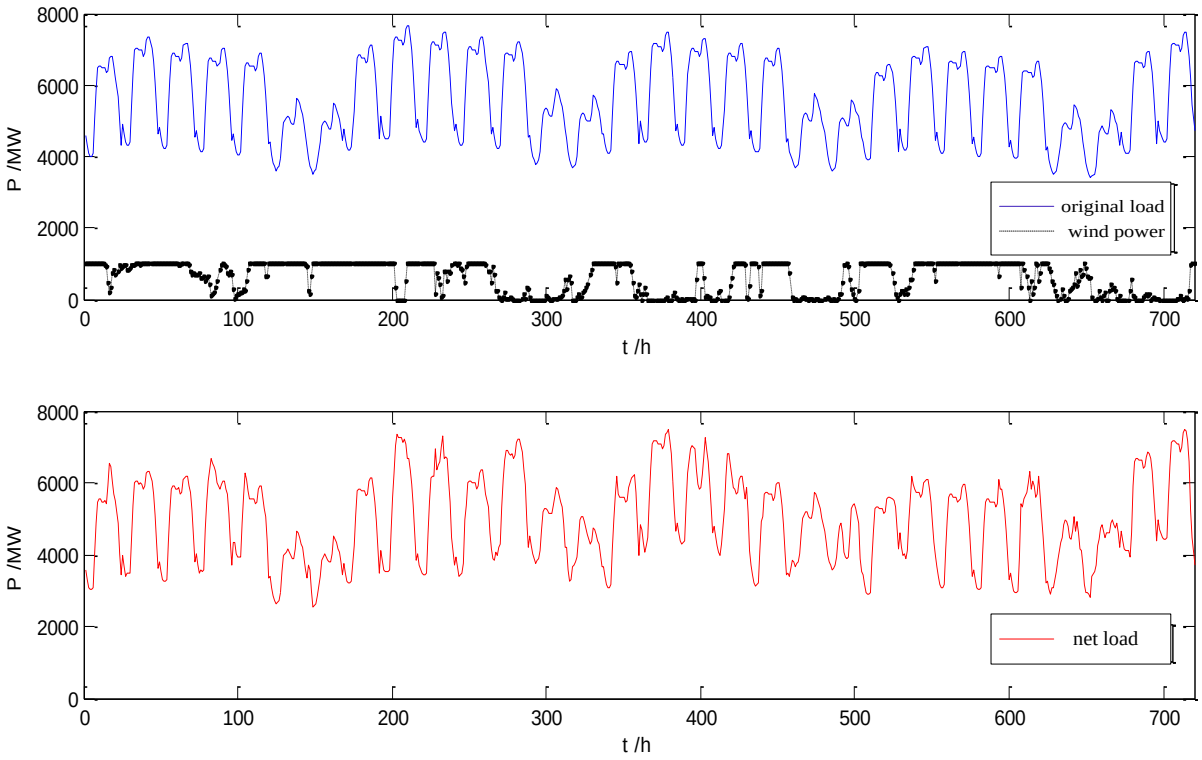

Fig. 4-1 IEEE RTS load date and wind power

Table 4-1 gives the parameter of wind turbines, the wind speed in the case is taken from

the example of the wind farm in Da Ban Cheng region. It is measured every ten minutes for one month and assume the average of six wind speeds every hour as the effective output in this hour. Then according to the principle of priority consumption of wind power, subtract the original system load from the wind power output, a net load sequence will be obtained, considering the wind power to be negative load.

Table 4-1 The parameter of wind turbines

Parameter	Value
Cut-in speed	3 [m/s]
Rated wind speed	10.3 [m/s]
Cut-out wind speed	22 [m/s]
Rated power	1.0 [MW]
Forced outage rate	0.05

4.1.2 Generator Data

Power generation system is using EPRI-36 test units with a total installed capacity of 8800MW. Unit reliability data and fuel cost is from the reference [48], the environmental cost data from reference [49], unit commitment and cost parameters reference [49] [50], the lack of electricity cost is set 1000 $/(MW h). The loading priorities is just the same as the sequence in Table 4-2. Among them, the first two units are the nuclear power units, which will take responsibility of the base load, and no factors of unit shutdown and startup is considered.

Table 4-2 The data of generator system EPRI-36

NO	Type	Capacity [MW]	Number of units	FOR	Minimum up time [h]	Minimum down time [h]	Unit cooling time constant [h]
1	nuclear power	1200	2	0.132	—	—	—
2	coal-fired	600	2	0.153	7	5	12
3	coal-fired	400	3	0.119	7	5	12
4	coal-fired	200	4	0.082	5	3	8
5	oil-fired	800	2	0.171	7	5	12

Table 4-2(continued) The data of generator system EPRI-36

NO	Type	Capacity [MW]	Number of units	FOR	Minimum up time [h]	Minimum down time [h]	Unit cooling time constant [h]
6	oil-fired	200	3	0.082	5	3	8
7	gas-fired	50	20	0.120	2	1	3

Table 4-2(continued) The data of generator system EPRI-36

NO	Type	Boiler startup cost [$/(MW time)]	Turbine startup cost [$/(MW time)]	Unit shutdown cost [$/(MW time)]	Fuel cost [$/(MW h)]	Environmental costs [$/(MW h)]
1	nuclear power	—	—	—	0.2	0.4
2	coal-fired	35	10	10	0.6	12
3	coal-fired	35	10	10	0.7	12
4	coal-fired	30	10	10	0.8	13
5	oil-fired	35	10	10	0.6	5
6	oil-fired	30	10	10	0.7	5.5
7	gas-fired	20	3	3	4	2.4

4.2 Result of Probabilistic Production Simulation

This thesis first simulates two scenarios for probabilistic production.

Scenario 1: original system without any wind power;

Scenario 2: penetrate 1000 numbers of wind turbines, i.e., 1000MW of the total installed wind power into the scenario 1 system, accounting for approximately 10.2% of the total system.

4.2.1 Analysis of Equivalent Interval Frequency Distribution

According to the method described in Section 3.1.1, step length Δx is set as 50MW. And scanning the net load curve point by point from the beginning, we can get the original interval-frequency distribution series. For convenience to describe, here the result of each load interval-frequency distribution series will be restored to the load frequency curve for analysis.

Fig. 4-2 is just the original restored equivalent load frequency curve and the load frequency curve obtained by FD method, you can see that these two curves are overlapped completely, indicating that the load interval-frequency distribution series can accurately restore the load frequency curve, It contains all the information load frequency curve.

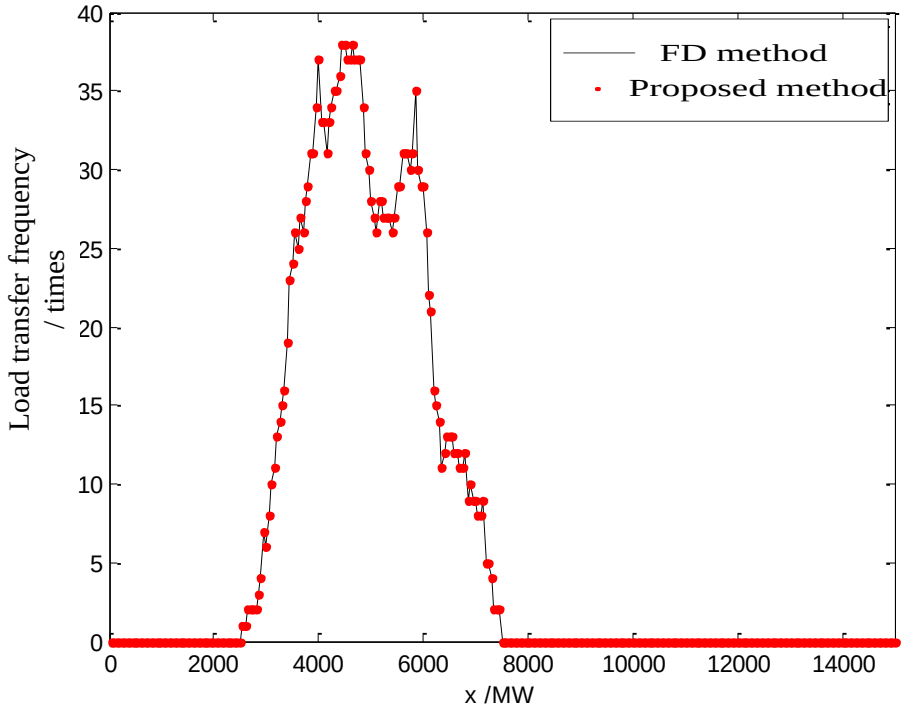

Fig. 4-2 The original load frequency curve

After penetrating the wind power as shown in Fig. 4-2, we can find that the system minimum load level in the study period 720 hours is 2500MW, the maximum load level is 7500MW. From the whole point of view, the load level ranging from 4000 ~5000MW have a relatively high transfer frequency and the corresponding units will meet a high frequent requirement of shutdown and startup, or adjustment of output operations. In the base load 0~2500MW, and the peak load 7000~7500MW, the operating units corresponds to the smaller load transfer frequency, the relative reduction will happen in the number of corresponding start and stop operation.

Loading units in the Table 4-2 one by one, each equivalent interval-frequency distribution series is restored into the load frequency curve according to formula (3-10). The process of convolution is shown in Fig. 4-3 and Fig. 4-4. Among them, the equivalent load frequency curve in FD method and the proposed method are exactly the same, which can verify the correctness of the proposed method. At the same time comparing these two different scenarios, we can find that for the average and maximum load transfer frequency Scenario 2 is always

greater than Scenario 1, which also confirms the degree of timing fluctuation is increased lot after considering intermittent wind power.

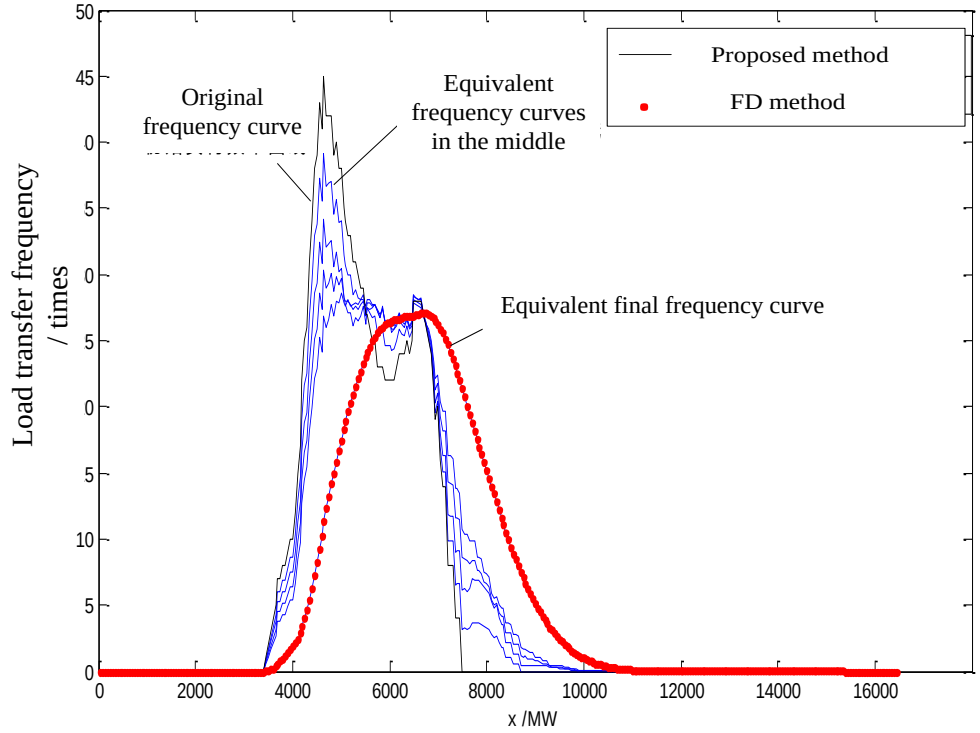

Fig. 4-3 The detailed convolution process without wind power

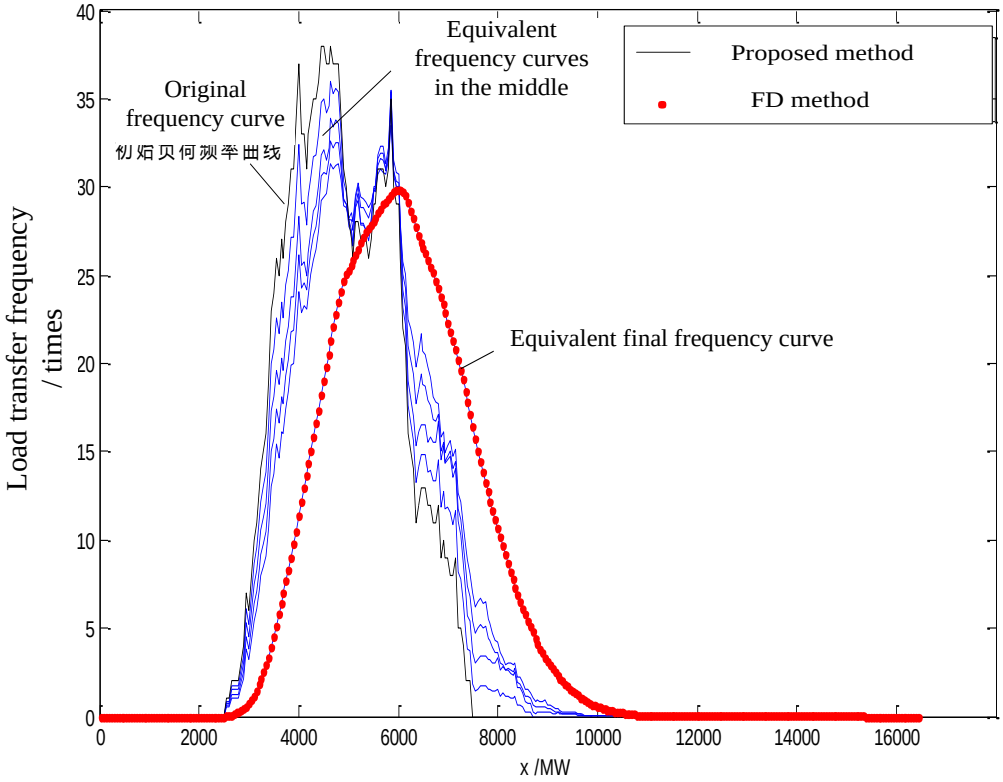

Fig. 4-4 The detailed convolution process with wind power

Here let's take the example of the 7-th unit for analysis, whose minimum up time is 7 hours, and minimum down time is 5 hours. And we can find that its loading position is just the sum of former 6 units capacity, which is equal to 4400MW.

Table 4-3 The equivalent interval-frequency distribution of 4400MW without wind power

$a^{(i-1=6)}_{(k=88,m,n)}$		$b^{(i-1=6)}_{(k=88,n,m)}$	
a(88,1,5)=1.258576	a(88,20,4)=1.829665	b(88,1,1)=1.678101	b(88,5,17)=3.356202
a(88,1,7)=0.419525	a(88,21,4)=0.427179	b(88,1,2)=0.839050	b(88,5,19)=0.264898
a(88,2,4)=0.839050	a(88,22,4)=0.151564	b(88,1,22)=0.151564	b(88,5,139)=0.113334
a(88,14,1)=0.419525	a(88,25,5)=0.419525	b(88,1,25)=0.419525	b(88,5,141)=0.151564
a(88,15,9)=0.419525	a(88,26,4)=0.419525	b(88,1,26)=0.419525	b(88,6,17)=0.113334
a(88,16,8)=0.419525	a(88,69,2)=0.419525	b(88,1,143)=0.007654	b(88,6,18)=0.113334
a(88,16,9)=0.419525	a(88,92,4)=0.113334	b(88,2,21)=0.427179	b(88,6,187)=0.151564
a(88,17,1)=2.936677	a(88,139,4)=0.113334	b(88,2,334)=0.007654	b(88,7,16)=0.839050
a(88,17,4)=0.419525	a(88,139,5)=0.264898	b(88,4,19)=2.056332	b(88,7,17)=0.952384
a(88,17,5)=0.839050	a(88,140,4)=0.151564	b(88,4,20)=1.829665	b(88,7,139)=0.113334
a(88,17,7)=0.646193	a(88,141,1)=0.151564	b(88,4,69)=0.419525	b(88,7,186)=0.113334
a(88,17,10)=0.419525	a(88,143,2)=0.007654	b(88,4,92)=0.113334	b(88,8,17)=0.419525
a(88,18,4)=0.113334	a(88,186,6)=0.113334	b(88,4,139)=0.151564	b(88,9,14)=0.419525
a(88,19,5)=1.103948	a(88,187,4)=0.151564	b(88,4,140)=0.151564	b(88,9,17)=0.419525
a(88,19,6)=0.264898	a(88,213,2)=0.007654	b(88,4,213)=0.007654	b(88,10,15)=0.419525
a(88,19,7)=0.952384	a(88,334,1)=0.007654		

Table 4-3 and Table 4-4 give the detailed equivalent interval-frequency distribution series for the load level 4400MW in two different Scenarios and correspond to spatial coordinate

system, as shown in Fig. 4-5 and Fig. 4-6. We can see clearly that the number of load transfers of short interval is greatly increased after integrating wind power, and the load transfer of which the upward duration is more than 7 hours and the corresponding downward duration is more than 5 hours is increased as well. It indicates that the volatility of wind power, not only brings more demand of shutdown and startup for generator, but also, more requests for the generator which cannot be accomplished. We need to eliminate this part of the short interval fluctuation impact in the dynamic cost evaluation.

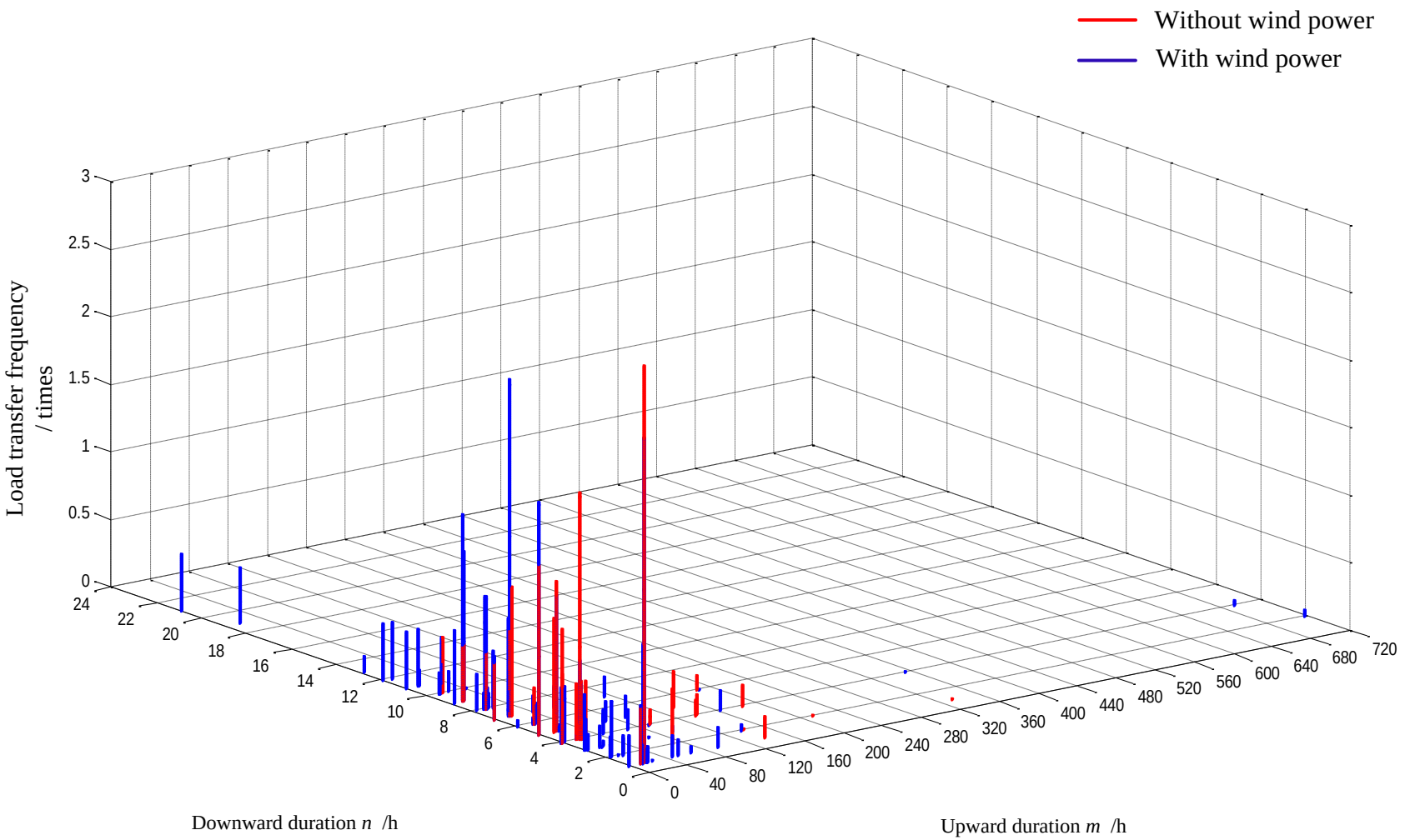

Fig. 4-5 The equivalent interval-frequency distribution $a^{(i-1=6)}_{(k=88,m,n)}$ of 4400MW with and without wind power

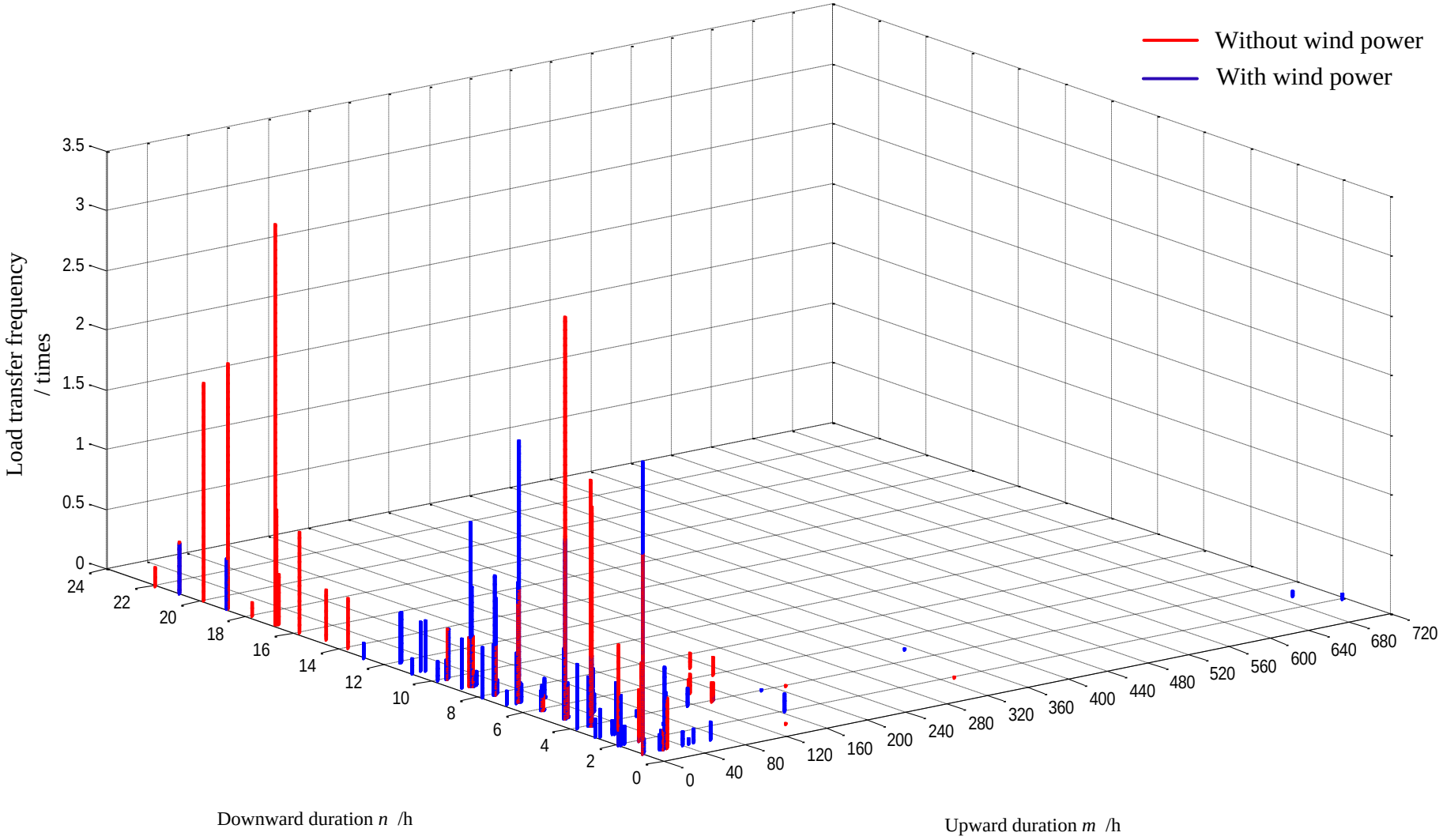

Fig. 4-6 The equivalent interval-frequency distribution $b^{(i-1=6)}_{(k=88,n,m)}$ of 4400MW with and without wind power

Table 4-4 The equivalent interval-frequency distribution of 4400MW with wind power

$a^{(i-1=6)}_{(k=88,m,n)}$		$b^{(i-1=6)}_{(k=88,n,m)}$	
a(88,1,1)=0.226667	a(88,19,1)=0.113334	b(88,1,1)=2.43838	b(88,4,19)=0.593355
a(88,1,4)=0.406184	a(88,19,2)=0.141287	b(88,2,1)=0.120988	b(88,5,19)=0.292851
a(88,1,5)=1.72329	a(88,19,5)=1.00231	b(88,3,1)=0.151564	b(88,6,19)=0.00276527
a(88,1,7)=0.468124	a(88,20,1)=0.0437099	b(88,13,1)=0.113334	b(88,7,19)=0.141287
a(88,2,3)=0.419525	a(88,20,3)=0.00765421	b(88,1,2)=0.627342	b(88,9,19)=0.113334
a(88,2,4)=0.166872	a(88,20,4)=0.57612	b(88,21,2)=0.419525	b(88,1,20)=0.151564
a(88,2,6)=0.0409446	a(88,20,6)=0.151564	b(88,1,3)=0.113334	b(88,3,20)=0.0409446
a(88,2,12)=0.419525	a(88,21,1)=0.113334	b(88,2,3)=0.419525	b(88,4,20)=0.578886
a(88,3,3)=0.226667	a(88,21,3)=0.0381682	b(88,11,3)=0.113334	b(88,5,20)=0.00765421
a(88,3,11)=0.419525	a(88,21,4)=0.419525	b(88,19,3)=0.419525	b(88,2,21)=0.0409446
a(88,3,21)=0.419525	a(88,21,5)=0.0485989	b(88,8,4)=0.419525	b(88,3,21)=0.427179
a(88,4,4)=0.419525	a(88,22,4)=0.00276527	b(88,7,5)=0.113334	b(88,4,21)=0.0381682
a(88,5,2)=0.151564	a(88,23,4)=0.113334	b(88,10,5)=0.151564	b(88,9,21)=0.113334
a(88,5,3)=0.113334	a(88,23,8)=0.419525	b(88,2,6)=0.151564	b(88,1,22)=0.00276527
a(88,6,8)=0.264898	a(88,23,10)=0.151564	b(88,3,6)=0.226667	b(88,1,23)=0.684423
a(88,6,9)=0.532859	a(88,26,1)=0.00765421	b(88,4,6)=0.532859	b(88,3,26)=0.00765421
a(88,6,13)=0.113334	a(88,41,7)=0.113334	b(88,9,7)=0.419525	b(88,1,41)=0.113334
a(88,7,2)=0.419525	a(88,41,10)=0.0076542	b(88,11,12)=0.419525	b(88,4,41)=0.00765421
a(88,12,12)=0.419525	a(88,42,6)=0.151564	b(88,7,14)=0.120988	b(88,7,42)=0.151564
a(88,14,1)=0.427179	a(88,43,5)=0.0485989	b(88,10,14)=0.159218	b(88,5,43)=0.0409446
a(88,14,2)=0.00765421	a(88,44,4)=0.182231	b(88,12,14)=0.419525	b(88,7,43)=0.00765421
a(88,14,8)=0.113334	a(88,46,1)=0.151564	b(88,7,15)=0.419525	b(88,5,44)=0.182231
a(88,14,10)=0.151564	a(88,47,5)=0.0409446	b(88,8,15)=0.419525	b(88,5,46)=0.151564
a(88,15,8)=0.83905	a(88,52,1)=0.113334	b(88,9,15)=1.37191	b(88,1,47)=0.0409446
a(88,15,9)=1.37191	a(88,63,7)=0.151564	b(88,10,15)=0.113334	b(88,1,52)=0.113334
a(88,15,10)=0.113334	a(88,65,1)=0.0409446	b(88,12,15)=0.419525	b(88,9,63)=0.151564
a(88,15,11)=0.419525	a(88,65,6)=0.00765421	b(88,5,16)=0.571089	b(88,4,65)=0.0409446
a(88,16,1)=0.879995	a(88,67,5)=0.0409446	b(88,6,16)=0.151564	b(88,7,65)=0.00765421
a(88,16,7)=0.722653	a(88,68,3)=0.00765421	b(88,7,16)=0.993329	b(88,6,67)=0.0409446
a(88,16,8)=0.83905	a(88,69,4)=0.141287	b(88,8,16)=0.990614	b(88,3,68)=0.00765421

Table 4-4(continued) The equivalent interval-frequency distribution of 4400MW with wind power

$a^{(i-1=6)}_{(k=88,m,n)}$		$b^{(i-1=6)}_{(k=88,n,m)}$	
a(88,16,9)=1.10395	a(88,69,5)=0.141287	b(88,9,16)=0.83905	b(88,1,69)=0.141287
a(88,16,10)=0.419525	a(88,90,5)=0.151564	b(88,10,16)=0.419525	b(88,5,69)=0.141287
a(88,16,19)=0.419525	a(88,91,4)=0.00765421	b(88,11,16)=0.419525	b(88,7,90)=0.151564
a(88,17,1)=2.40202	a(88,92,3)=0.0409446	b(88,3,17)=0.113334	b(88,5,91)=0.00765421
a(88,17,4)=0.0409446	a(88,92,4)=0.00276527	b(88,4,17)=0.419525	b(88,4,92)=0.00276527
a(88,17,7)=2.49847	a(88,93,1)=0.141287	b(88,5,17)=1.49365	b(88,5,92)=0.0409446
a(88,17,8)=0.159218	a(88,115,7)=0.141287	b(88,6,17)=0.200163	b(88,4,93)=0.141287
a(88,17,11)=0.113334	a(88,140,2)=0.0409446	b(88,7,17)=2.18191	b(88,4,115)=0.141287
a(88,18,2)=0.113334	a(88,165,4)=0.141287	b(88,8,17)=0.805411	b(88,4,140)=0.0409446
a(88,18,3)=0.159218	a(88,189,6)=0.0027652	b(88,1,18)=0.120988	b(88,2,165)=0.141287
a(88,18,6)=0.0409446	a(88,354,4)=0.0027652	b(88,4,18)=0.120988	b(88,4,189)=0.0027652
a(88,18,7)=0.347655	a(88,692,4)=0.0381682	b(88,5,18)=0.264898	b(88,5,354)=0.0027652
a(88,18,8)=0.113334	a(88,718,2)=0.0460978	b(88,7,18)=0.154278	b(88,3,692)=0.0381682
		b(88,8,18)=0.113334	b(88,2,718)=0.0460978
		b(88,1,19)=0.113334	

According to the formula (3-8) and (3-13), select the satisfied time structure to calculate the frequency of startup and shutdown frequency and we can obtain the following Table 4-5. Comparing these two different scenarios, the total upward and downward transfer are both increased approximately by 60% and for the first type of time structure of short interval is increased by 26.8%, the second type is 31.9%.

Table 4-5 The statistics of equivalent time structure of 4400MW

Scenario	$a^{(i-1=6)}_{(k=88,m,n)}$			$b^{(i-1=6)}_{(k=88,n,m)}$		
	Downward transfer	Short time interval	Expected shutdown frequency	Upward transfer	Short time interval	Expected startup frequency
Scenario 1	14.66	9.13	5.53	14.66	7.65	7.01
scenario 2	23.47	12.03	11.43	23. 47	9.70	13.77

At the same time we can also find that here is about more than 50% belonging to the short time interval in both kinds of time structures, which is not in accordance with the requirements of the appropriate unit startup and shutdown. If this kind of time structure is eliminated, it will introduce significant errors during dynamic cost evaluation.

4.2.2 Analysis of Probabilistic Production Simulation

Table 4-6 The comparison of unit expected energy with wind power

Unit	Expected energy of *i-th* unit E_{g_i} (MW h)		Unit	Expected energy of *i-th* unit E_{g_i} (MW h)	
	Proposed method	EEF method		Proposed method	EEF method
1	749952	749952	*19*	3009.73	3104.55
2	749952	749952	*20*	2848.59	2947.21
3	363032	363426	*21*	2707.75	2784.81
4	343412	344736	*22*	2547.68	2633.26
5	221050	222224	*23*	2405.93	2489.17
6	202051	203442	*24*	2275.18	2354.67
7	182622	184087	*25*	2154.04	2221.97
8	87955	88756.6	*26*	2026.48	2095.64
9	82713.5	83429.6	*27*	1904.75	1973.9
10	77259.5	78031.8	*28*	1790.6	1858.35
11	71347.9	72251.5	*29*	1686.22	1746.98
12	193811	197078	*30*	1583.82	1641.12
13	118737	121345	*31*	1485.13	1540.65
14	23446.9	24042.4	*32*	1392.07	1445.96
15	19358.9	19891.2	*33*	1305.74	1355.66
16	15865	16318.4	*34*	1222.69	1269.36
17	3375.21	3450.34	*35*	1142.54	1187.17
18	3160.58	3278.26	*36*	1066.83	1109.8

Table 4-7 The comparison of reliability index with wind power

Index	Proposed method	EEF method
Original system load E_D [10^4MW h]	351.35	353.16
EENS [10^4MW h]	1.3192	1.3796
LOLP	0.0337	0.0341

Table 4-6 and Table 4-7 give the result of expected energy of each unit and reliability

index with wind power in EEF method and proposed method. Not difficult to find, the desirable energy for each unit is similar to each other and the reliability index is similar as well, which can verify the correctness of the proposed method in generating energy and reliability assessment.

4.3 Assessment of Dynamic Costs

4.3.1 Analysis of Generator Expected Startup and Shutdown Frequency

For the expected startup and shutdown frequency of units, this thesis employs the FD method and proposed method for comparison. In the proposed algorithm, it is also calculated in case of no elimination. The detailed results are given in Table 4-8. First of all, we can find that the startup and shutdown frequency in the proposed method is decreased respectively, 30.2%, 34.6% compared with the one in FD method after removing the time structure of short time interval. In the other words, the eliminated time structures is taking up almost one third in the total distribution. If it includes the time structures of short time interval, the result is fully consistent with the one in FD method, which can demonstrate the validity of the proposed algorithm once again.

Table 4-8 The expected startup frequency of each unit

Unit	Proposed method		FD method
	Include short time interval	Exclude short time interval	
1	0	0	0
2	0	0	0
3	0	0	0
4	1.08	3.24	3.24
5	6.06	12.94	12.94
6	9.79	20.22	20.22
7	13.77	23.47	23.47
8	19.68	27.54	27.54
9	19.9	26.5	26.5
10	20.78	27.72	27.72
11	20.55	26.73	26.73
12	15.14	24.99	24.99
13	10.79	20.93	20.93
14	8.69	16.7	16.7
15	7.48	14.37	14.37
16	6.13	12.27	12.27
17	8.55	10.04	10.04

Table 4-8(continued) The expected startup frequency of each unit

Unit	Proposed method		FD method
	Include short time interval	Exclude short time interval	
18	8.31	9.82	9.82
19	7.99	9.29	9.29
20	7.69297	8.91397	8.91397
23	6.57	7.78	7.78
24	6.3	7.37	7.37
25	5.98	7.01	7.01
26	5.65	6.71	6.71
27	5.36	6.38	6.38
28	5.12	6.06	6.06
29	4.85	5.74	5.74
30	4.57	5.46	5.46
31	4.32	5.18	5.18
32	4.09	4.91	4.91
33	3.88	4.63	4.63
34	3.65	4.38	4.38
35	3.42	4.13	4.13
36	3.22	3.89	3.89

Table 4-9 The expected shutdown frequency of each unit

Unit	Proposed method		FD method
	Include short time interval	Exclude short time interval	
1	0	0	0
2	0	0	0
3	0	0	0
4	1.08	3.24	3.24
5	5.11	12.94	12.94
6	7.81	20.22	20.22
7	11.43	23.47	23.47
8	16.46	27.54	27.54
9	18.24	26.50	26.50
10	18.96	27.72	27.72
11	18.80	26.73	26.73
12	14.23	24.99	24.99
13	10.32	20.93	20.93
14	7.93	16.70	16.70
15	6.82	14.37	14.37
16	5.64	12.27	12.27
17	8.55	10.04	10.04

Table 4-9(continued) The expected shutdown frequency of each unit

Unit	Proposed method		FD method
	Include short time interval	Exclude short time interval	
18	8.31	9.82	9.82
19	7.99	9.29	9.29
20	7.69	8.91	8.91
21	7.24	8.52	8.52
22	6.88	8.18	8.18
23	6.57	7.78	7.78
24	6.3	7.37	7.37
25	5.98	7.01	7.01
26	5.65	6.71	6.71
27	5.36	6.38	6.38
28	5.12	6.06	6.06
29	4.85	5.74	5.74
30	4.57	5.45	5.45
31	4.32	5.18	5.18
32	4.09	4.91	4.91
33	3.88	4.63	4.63
34	3.65	4.38	4.38
35	3.42	4.13	4.13
36	3.22	3.89	3.89

4.3.2 Analysis of Dynamic Costs

Table 4-10 The comparison of each dynamic cost index

Dynamic cost index	Proposed method		FD method
	Include short time interval	Include short time interval	
I_{FGSUC}	12.94	22.37	22.37
C_{TSU} [10^5\$]	5.56	8.17	8.17
C_{BSU} [10^6\$]	1.13	1.65	2.59
C_{sd} [10^5\$]	5.03	8.17	8.17
C_d [10^5\$]	21.85	32.83	42.28

Table 4-10 gives the specific dynamic costs of each index. Due to the exclusion of the time structure of short interval, the final dynamic costs in the proposed method, is decreased

by 48.2% compared with the one in FD method. In the case of no elimination in proposed method, each index is exactly the same with the one in FD method, except for the boiler startup cost, since the offline time for each startup is directly the average in FD method, while in proposed method, it is the corresponding downward duration for the exact offline time. It can also show the correctness of this proposed method.

In order to evaluate the impact of short term fluctuations in the time structure, the Short Time Interval Dynamic Cost I_{STIDC} is induced and the result is as follows.

$$I_{\mathrm{STIDC}} = \frac{C_d^{'} - C_d}{C_d^{'}} = \frac{32.83\text{-}21.85}{32.83} = 33.5\% \tag{3-27}$$

Eliminating these time structures of short interval, will result in the factor that it needs to keep some units in the state of standby, which will have an economic effect to some extent. Here the Short Time Interval Proportion of Unit Capacity I_{STIPUC} is induced to reflect this part influence from the point of view of the proportion of the total time and calculated as follows.

$$I_{\mathrm{STIPUC}} = \frac{\frac{1}{T}\sum_{i=1}^{n} C_i \left(T_i^{start} + T_i^{end}\right)}{\sum_{i=1}^{n} C_i} = 9.429 \tag{3-28}$$

Table 4-11 Probabilistic production simulation results based on interval-frequency distribution

Production cost	Scenario 1	Scenario 2
Original system load [10^4MW ћ]	399.32	351.35
EENS [10^4MW ћ]	3.0035	1.3192
LOLP	0.0727	0.0337
Dynamic cost C_d [10^6\$]	2.07	2.18
Fuel cost cC_d [10^6\$]	2.22	1.80
Environmental cost C_{envi} [10^7\$]	2.51	2.19
Customer interruption cost C_{voll} [10^7\$]	3.00	1.32
Total cost C_{total} [10^7\$]	5.95	3.91

Table 4-11 shows the probabilistic production simulation results in different scenarios. With the wind power, the EENS is decreased by 56% and LOLP is reduced by 53.66%, indicating that wind power will help to improve the reliability of original power system. For the fuel cost, it saves by 18.9% and the environmental cost is decreased by 12.8%, the customer interruption cost is also reduced 56%. Meanwhile, the preventable costs of wind power is 2.0455×10^7 \$, the total production cost saves by 34.3% with wind power.

4.3.3 The Influence of Wind Capacity

To further investigate how the wind power capacity affects the results, we compare the evaluation in different penetration scenarios of wind power ranging from 0~1500MW, especially for the short time interval dynamic cost I_{STIDC}, short time interval proportion of unit capacity I_{STIPUC} and the dynamic cost rate η.

$$\eta=\frac{C_d}{C_{total}}\times100\% \tag{3-29}$$

Where:

C_d ——dynamic cost in the proposed method;

C_{total} ——the total production cost.

The relationship between the dynamic cost index and the number of wind turbines is shown in Fig. 4-7 and Fig. 4-8. It can be seen, both the short interval dynamic cost and short time interval proportion of unit capacity trend to grow with the increasing amount of wind power integration, which is consistent with the increased volatility and with the increased effect caused by the short time interval fluctuations.

At the same time, there is a partial decline phenomenon of the dynamic cost with the increasing wind power integration. This is mainly because the loading position of each unit is changed by the different of volatility of wind power. The corresponding required unit shutdown and startup will also change since the strongest fluctuated load interval varies with different penetration of wind power.

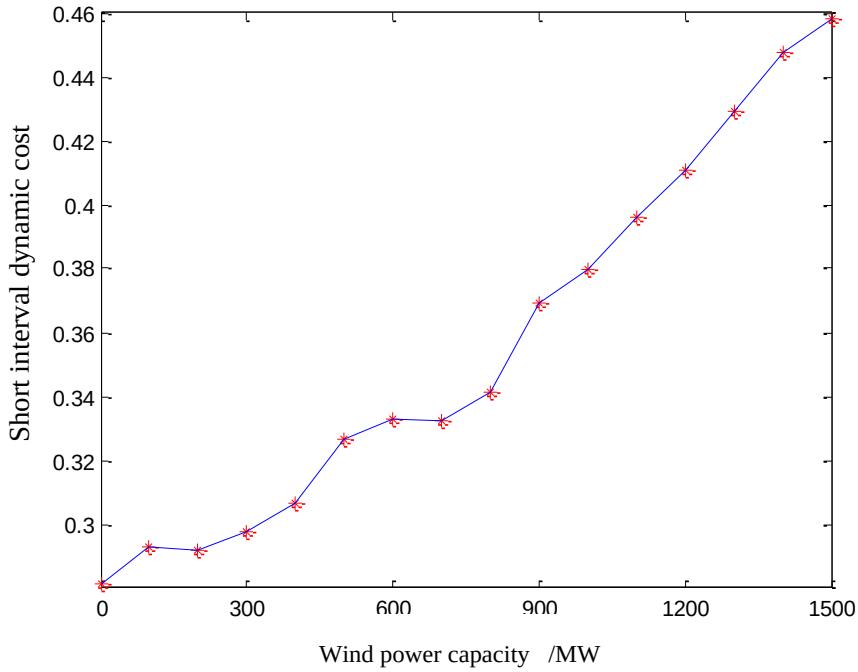

Fig. 4-7 The relationship between short interval dynamic cost and the number of wind turbines

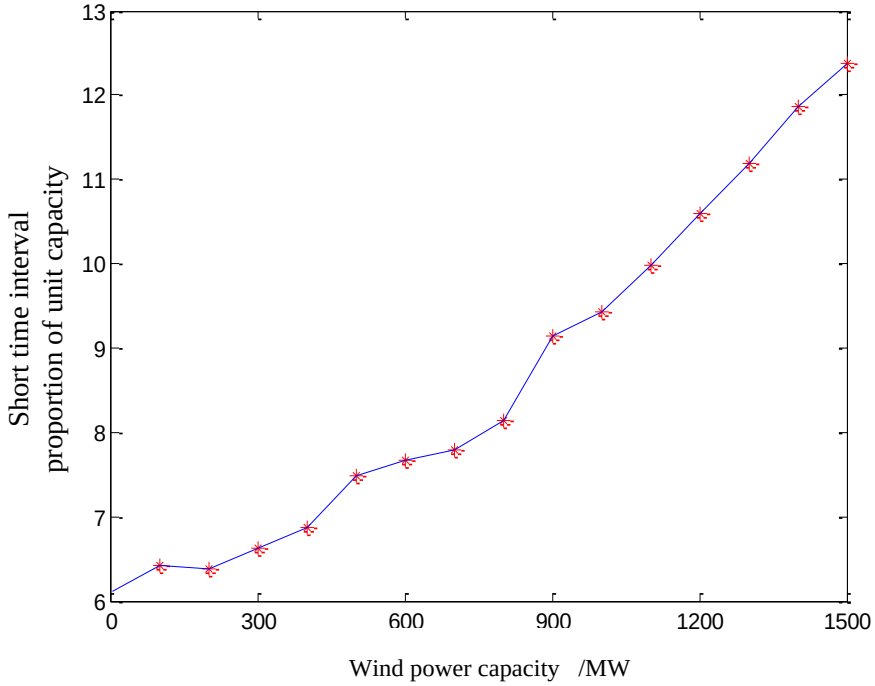

Fig. 4-8 The relationship between short time interval proportion of unit capacity and the number of wind turbines

As shown in Fig. 4-9, the dynamic cost rate is only 3.64%without any wind power. When it is penetrated 700MW of wind power, the dynamic cost rate is growing into 5.17%; and when the wind farm installed capacity is increased to 1500MW, the dynamic cost rate will become

as high as 6.1%. Obviously, with increasing wind power installed capacity, dynamic cost rate will be gradually increased. Hence to some extent, during the wind farm planning, we can take advantage of this proposed algorithm to determine the appropriate scale of penetrated wind power based on the expected dynamic cost rate.

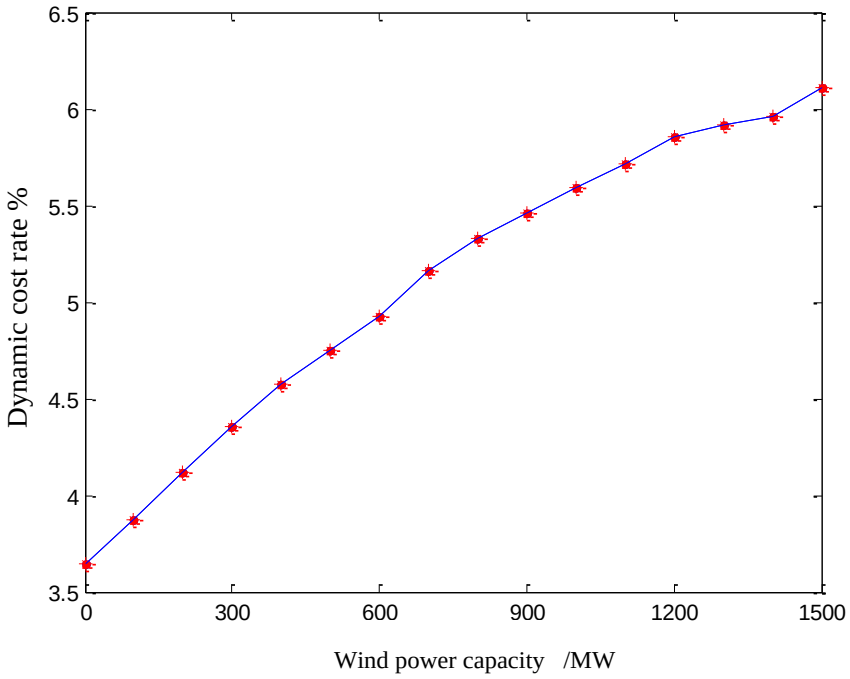

Fig. 4-9 The relationship between dynamic cost rate and the number of wind turbines

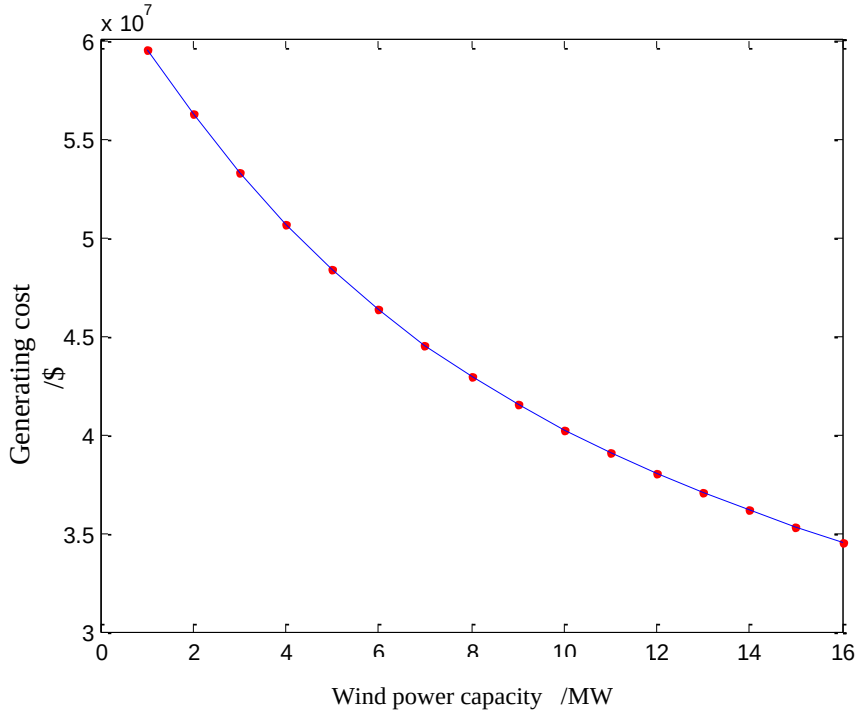

Fig. 4-10 The relationship between generating cost and the number of wind turbines

5 Conclusions

With the increasing penetration of wind power into the grid, probabilistic production simulation with the coexistence of multiple energy intermittent is playing an important role in the plan and operation, reliability assessment and spare capacity determination of power system. Therefore, it is significantly meaningful in the wind power grid integration to study and discuss about the probability production simulation including wind farms. Generally speaking, the traditional methods, neglect the timing fluctuation of system load, resulting in the fact that it fails to include the dynamic costs related to the minimum up-time time or minimum down-time time limits, ramping rate restriction, generator scheduling, and other factors in the production simulation process. The final production cost is relatively sketchy. With the growing amounts of the intermittent energy, such as wind power, the volatility of power system is further improved, the unit shutdown and startup operation is becoming more frequently and the dynamic cost is also increased a lot. This thesis extends the load frequency curve into the interval frequency distribution series which contains both the load fluctuation frequency information and timing distribution information. Based on this series, a new kind of method has been developed to evaluate the frequency of startup and shutdown operation and get a more reasonable assessment of dynamic costs, which can be better applied to a comprehensive assessment of the power system production costs. The main research achievement can be summarized as the following three points.

(1) First of all, aiming at describe the load timing volatility, the interval-frequency distribution series is expanded based on load transfer from the load frequency curve. Not only it can reflect the fluctuation frequency information, but also it can record the timing distribution of each load transfer in the form of time structure. Meanwhile, this kind of series can be completely accurately restore to the corresponding load frequency curve. there exists a certain reference value in characterizing the timing characteristics of the system load.

(2) Analog to the traditional probabilistic production simulation, we employ the standard convolution to consider the unit random failure as the modification of each time structure in the original interval-frequency distribution series. In this way, both the fluctuation frequency information and timing distribution can be taken into account in the simulation process. Then based on the detailed information inside the structure in the equivalent

distribution series, the expected energy of each power generating units and reliability analysis is evaluated, and compared with the classical equivalent energy function method, the difference is not that big, which demonstrates its validity from this point of view.

(3) For the evaluation of dynamic cost, it is assumed that the request of unit shutdown due to load downward transfer will be fulfilled only when its adjacent two time intervals are larger than the minimum up time and minimum down time limits, respectively. Similarly, the request of unit startup due to load upward transfer will be fulfilled only when its adjacent two time intervals are larger than the minimum down time and minimum up time limits. With this assumption to consider the infeasibility of startup and shutdown in a short time interval, we can get a more rational assessment for the unit shutdown and startup frequency, compared with the one in frequency and duration method. The related dynamic cost is more close to the actual system conditions.

With the increasing penetration of wind power, more impact will be produced by the growing volatility. The proportion of short time interval in the interval frequency distribution series is increasing dramatically, affecting the assessment dynamic costs a lot. It’s worthy to be considered in the simulation process The proposed method can be combined with other applications to apply for the comprehensive evaluation of production costing and the effect of wind farm installed capacity.

References

[1] Wang Xifan. Power system optimization planning[M]. China Hydraulic Engineering Press, 1990.

[2] Liu Zhenya. China Electric Power and Energy[M]. China Electric Power Press, 2012.

[3] Zhoutian Rui, Wang Xu, Zhang Qian, et al. Analysis of related problems with a large scale wind farm penetration in Jilin Province[J]. Journal of China Electric Power, 2008, 36 (3): 1-3,8.

[4] Zhoutian Rui, Wang Xu, Zhang Qian, et al. Empirical Analysis of the influence of planning large-scale wind power in Jiangsu Power Grid [J]. Journal of China Electric Power, 2010, 43 (2): 11-15.

[5] The grid technology (training) center of Northwest Power Grid Co., Ltd., the Wind Power Research Center of Northwest Power Grid Co., Ltd.. Northwest (Jiuquan) wind power output characteristics[R]. Northwest Power Grid Co., Ltd., 2008.

[6] China Electricity Enterprise Council. China Power Industry Status and Prospects[OL]. http://www.cec.org.cn/yaowenkuaidi/2015-03-10/134972.html.

[7] Wei Xianfei. The current status and prospect of wind power development. Journal of Business Economics, 2010,364 (12): 21-23.

[8] Xiao Chong Ying, Wang Ning Bo, Ding Kun, Zhi Jing. Gansu Jiuquan wind power adjustment mode [J]. Proceedings of the CSEE, 2010,30 (10): 1-7.

[9] Xiao Chong Ying, Wang Ning Bo, Zhi Jing, Ding Kun. Jiuquan wind power output characteristic analysis [J]. Journal of Electric Power System and its Automation, 2010,17: 64-67.

[10] Zhang Ning, Zhou Tianrui, Duan Changgang, and so on. The impact of large-scale wind farms on the power system peaking regulation [J]. Journal of Power System Technology, 2010,34 (1): 152-158.

[11] Sun Rongfu, Zhang Tao, Liang Ji. Assessment and application of wind power capacity acceptance [J]. Journal of electric power system and its automation, 2011 (4): 70-76.

[12] Han Xiaoqi, Sun Shouguang, Qiqing Ru. Assessment from the system point of view grid peaking acceptance of wind power capacity [J]. Journal of China Electric Power, 2010,43 (6): 16-19.

[13] Xinjiang Electric Power Company. Preliminary analysis of the impact of Da Bancheng wind power in Urumqi power grid operation [J]. Journal of China Wind power, 998, (3): 23-25.

[14] Liu Hong. A preliminary study proportion of allowed wind power in Urumqi grid[J]. Journal of China Wind power, 1999, (15): 28-29.

[15] Booth R R. Power system simulation model based on probability analysis[J]. IEEE Transactions on 91.1(1972):62-69.

[16] Billinton R, Li W. A Monte Carlo method for multi-area generation system reliability assessment[J]. IEEE Transactions on Power Systems,1992,7(4):1487-1492.

[17] Stremel J, Jenkins R, Babb R, et al. Production costing using the cumulant method of representing the equivalent load curve[J]. IEEE Transactions on Power Apparatus and Systems, 1980, 5(PAS-99): 1947-1956.

[18] Rau N S, Toy P, Schenk K F. Expected energy production costs by the method of moments[J]. Power Apparatus and Systems, IEEE Transactions on, 1980 (5): 1908-1917.

[19] Wang Xifan. Fundamental of Power system optimization planning[M]. China Electric Power Press, 1994: 64-95.

[20] Wang Xifan. EEF approach to power system probabilistic modeling [J]. Journal of Xi’an Jiaotong University, 1984, 18(6): 13-26.

[21] Wang X. Equivalent energy function approach to power system probabilistic modeling[J]. IEEE

Transactions on Power Systems,1988,3(3):823-829.
[22] Xia Qing, Wang Shaojun, Xiang Niande. The probabilistic power system production simulation based on chronological load curve [J]. Proceedings of the CSEE, 1994, 14(3): 21-28.
[23] Xia Qing, Wang Shaojun, Xiang Niande. The probabilistic power system production simulation based on chronological load curve [J]. Proceedings of the CSEE, 1998, 18(6): 429-433.
[24] Liao Yuhan. Probabilistic production simulation with wind farms and application [D]. North China Electric Power University, 2012.
[25] Shi Wenhui, Chen Jing, Wang Weisheng. Reliability Assessment of interconnected power system with wind farms [J]. Journal of Power System Technology, 2012,36 (2): 224-230.
[26] Liu Xu. Stochastic production costing with wind farms [D]. Shandong University, 2013.
[27] Wang Xifan, Wang Xiuli. Probabilistic production simulation method and its application[J]. Journal of Electric Power System and its Automation,, 2003, 27(8): 10-15.
[28] Zou Bin, Li Dong. Power system probabilistic production simulation with wind generation based on available capacity distribution[J]. Proceedings of the CSEE, 2012, 32(7): 23-31.
[29] Zhang Ning, Kang Chongqing, Chih Chen Ping, et al. Wind power trusted capacity calculation method based on computing sequence [J]. Proceedings of the CSEE, 2011,31 (25): 1-9.
[30] Hu Guowei, Bie Zhaohong, Wang Xifan. Optimal dispatch in wind integrated system considering operation reliability[J]. Transactions of China Electrotechnical Society, 2013, 28(5): 58-65.
[31] Chen Shuyong, Dai Huizhu. Stochastic production costing with wind farms [J]. Journal of China Electric Power, 2000,33 (3): 30-31.
[32] Zhang Ningyu, Gao Shan, Zhao Xin. An unit commitment model and algorithm with randomness of wind power[J]. Transactions of China Electrotechnical Society, 2013, 28(5): 22-29.
[33] Grubb, Michael. The inclusion of dynamic factors in statistical power system cost models. I. Assessment of startup and banking costs[J]. Power Systems, IEEE Transactions on 4.2 (1989): 419-425.
[34] Grubb, Michael. The inclusion of dynamic factors in statistical power system cost models. II. Part loading and reserve costs[J]. Power Systems, IEEE Transactions on 4.2 (1989): 524-529.
[35] Arif S. Malik, Brian J. Cory. An application of frequency and duration approach in generation planning[J]. Power Systems, IEEE Transactions on 12.3 (1997): 1076-1084.
[36] Malik, A. S. Simulating limited energy units within the framework of ELDC and FD methods[J]. International journal of electrical power & energy systems 26.8 (2004): 645-653.
[37] Zhang Jietan, Cheng Haozhong, Hu Zechun, et al. Power system probabilistic production simulation including wind farms[J]. Proceedings of the CSEE, 2009, 29(28): 34-39.
[38] Qu Chong, Wang Xiuli, Xie Shaoyu, et al. Improved algorithm for probabilistic production simulation of power systems with wind power[J]. Journal of Xi’an Jiaotong University, 2012, 46(6).
[39] Yuan Jiandang, Yuan Tiejiang, Chao Qin, Li Yiyan. Study of generation expansion planning of the power system incorporating large-scale wind power in the environment of electricity market[J]. Power System Protection and Control, 2013, 28(5): 22-29.
[40] Lei Yazhou, Wang Weisheng, Yin Yonghua, et al. Analysis of wind power value to power system operation[J]. Power System Technology, 2002, 26(5): 10-14.
[41] Liu Jin, Yu Jilai, Liu Zhuo. An intelligent optimal dispatch strategy for spinning reserve coping with wind intermittent disturbance[J]. Proceedings of the CSEE, 2013, 33(1): 163-170.
[42] Tuoh Y. A., Meibom P., Denny E., et al. Unit commitment for systems with significant wind penetration[J]. IEEE trans on power systems, 2009, 24(2): 592-60.
[43] Nakamura S.. A review of electric production simulation and capacity expansion planning programs[J], Energy research, Vol. 8,231-240, 1984.
[44] Palsson M., Uhlen K,T. Oftevaag T et al. Large-scale wind power integration and voltage stability

limits in regional networks[C]. IEEE power engineering society summer meeting, Chicago, USA, 2000: 762-769.

[45] Wiik J., Gjengedal T.,Gjerde J.O., et al. Steady state Power system issues when Planning large wind farms[C]. IEEE power engineering society winter meeting, 2004,1: 199-204.

[46] Amora M. A. B.,Bezerra U. H.. Assessment of the effects of wind farms connected in a power system[C]. Power tech proceedings, 2011 IEEE porto.,4: 6.

[47] Tande J. 0.G., Uhlen K.. Wind turbines in weak grids-constraints and solutions[C]. 16th international conference and exhibition on electricity distribution part 1: contributions and summaries, 2006: 261.

[48] The Reliability Test System Task Force of the Application of Probability Methods Subcommittee. IEEE Reliability Test System [J]. IEEE Transactions on Power Apparatus and Systems, 1979, 98(6) : 2047-2054.

[49] Hall, J. D., R. J. Ringlee, and A. J. Wood. Frequency and duration methods for power system reliability calculations: I-Generation system model[J]. Power Apparatus and Systems, IEEE Transactions on 9 (1968): 1787-1796.

[50] Ringlee, Robert J., and Allen J. Wood. Frequency and duration methods for power system reliability calculations: II-Demand model and capacity reserve model[J]. Power Apparatus and Systems, IEEE Transactions on 4 (1969): 375-388.

[51] Galloway, CHARLES D., et al. Frequency and Duration Methods for Power System Reliability Calculations Part III: Generation System Planning[J]. Power Apparatus and Systems, IEEE Transactions on 8 (1969): 1216-1223.

[52] Ringlee, Robert J., and Allen J. Wood. Frequency and Duration Methods for Power System Reliability Calculations, Part V: Models for Delays in Unit Installations and Two Interconnected Systems[J]. Power Apparatus and Systems, IEEE Transactions on 1 (1971): 79-88.

[53] Hasche, B. Keane, A,O'Malley, M. Capacity Value of Wind Power, Calculation, and Data Requirements: the Irish Power System Case[J]. IEEE Transactions on Power Systems, 2011,26(1): 420-430.

[54] Dobakhshari A S, Fotuhi-Firuzabad M. A reliability model of large wind farms for power system adequacy studies[J]. IEEE Transactions on Energy Conversion, 2009, 24(3): 792-801.

[55] Xie Kaigui. Considering wind speed correlation of WECS in reliability evaluation using the time-shifting[J]. Electric Power system Research, 2009, 79(4): 687-693.

[56] Ning Zhang, Chongqing Kang, et al. Simulationmethodology of multiple wind farms operation considering wind speedcorrelation[J]. International Journal of Power and Energry System, 2010, 4(30): 264-27.

Research Achievements during the study

[1] 金烂聚，王秀丽，等．高压直流输电谐波保护综述[C]．中国高等学校电力系统及其自动化专业第三十届学术年会．北京：北京交通大学，2014．

[2] Linhong, Xie, Lanju Jin, Xiuli Wang, et al. Improved Protection Method of HVDC Transmission Line Based on the Analysis of Traveling Wave Dispersion [C]. CSEE and IEEE PES International Conference on Power System Technology. Chengdu, China on October, 2014:467~473 (DOI: 10.1109/POWERCON.2014.6993712).

[3] Lanju Jin, Xiuli Wang, et al. Power System Probabilistic Production Simulation Based on Equivalent Interval Frequency Distribution Including Wind Farms[C]. CSEE and IEEE PES International Conference on Power System Technology. Chengdu, China on October, 2014:336~342 (DOI: 10.1109/POWERCON.2014.6993631).

[4] Lanju Jin, Wenhui Shi, et al. An improved algorithm for Power System Probabilistic Production Simulation Based on Equivalent Interval Frequency Distribution[C]. IEEE PES Asia-Pacific Power and Energy Engineering Conference. Hong Kong, China on December, 2014:1~4 (DOI:10.1109/APPEEC.2014.7066154).